Vesicles and vesicle gels - structure and dynamics of formation

2003 J. Phys.: Condens. Matter 15 R655

(http://iopscience.iop.org/0953-8984/15/19/202)

INSTITUTE OF PHYSICS PUBLISHING JOURNAL OF PHYSICS: CONDENSED MATTER

J. Phys.: Condens. Matter **15** (2003) R655–R697 PII: S0953-8984(03)25666-6

TOPICAL REVIEW

Vesicles and vesicle gels—structure and dynamics of formation

M Gradzielski

Lehrstuhl für Physikalische Chemie I, Universität Bayreuth, D-95440 Bayreuth, Germany

Received 4 December 2002
Published 6 May 2003
Online at stacks.iop.org/JPhysCM/15/R655

Abstract

Vesicles constitute an interesting morphology formed by self-aggregating amphiphilic molecules. They exhibit a rich structural variety and are of interest both from a fundamental point of view (for studying closed bilayer systems) and from a practical point of view (whenever one is interested in the encapsulation of active molecules). In many circumstances vesicular structures have to be formed by external forces, but of great interest are amphiphilic systems, where they form spontaneously. Here the question arises of whether this means that they are also thermodynamically stable structures, which at least in some systems appears to be the case. If such vesicles are well defined in size, it is possible to pack them densely and thereby form vesicle gels that possess highly elastic properties even for relatively low volume fractions of amphiphile. Conditions for the formation and the microstructure of such vesicle gels have been studied in some detail for the case of unilamellar vesicles. Another important and topical issue is the dynamics of vesicle formation/breakdown, as the understanding of the transition process will open the way to a deeper understanding of their stability and also allow controlling of the structures formed, by means of their formation processes. Significant progress in the study of the transformation processes has been achieved, in particular by means of time-resolved scattering experiments.

(Some figures in this article are in colour only in the electronic version)

Contents

1. Introduction

Amphiphilic molecules (due to their surface-active properties, also called surfactants) are composed of a hydrophobic part and a hydrophilic head group. Due to this dual character they self-assemble in aqueous solution in a variety of morphologically different structures [1–5]. The driving force for this aggregation process is the tendency of the hydrophobic part to minimize contact with water, an effect called the hydrophobic effect and that is mainly due to the entropic gain of the water structure by not being in contact with the hydrophobic part [6]. A variety of different aggregate shapes are observed that range from spherical and rod-like micelles to amphiphilic bilayers. The actual form assumed by an aggregate depends on the molecular constitution of the amphiphile and can be explained by simple geometric consideration. In a first-order approximation the geometry of an amphiphile is described by the packing parameter p of the amphiphile, which is defined as the ratio of the hydrophobic volume (v_s) to the product of the head group area (a_s) and chain length l_s) [7]:

$$p = v_s/(a_s l_s). \tag{1}$$

The packing parameter determines the preferred curvature of the aggregates formed (cf figure 1). In forming space-filling aggregates, for $p < 1/3$ spherical objects, for $1/3 < p < 1/2$ rod-like particles, and for $1/2 < p$ bilayer structures are expected, while for values of p larger than 2, reverse structures should be formed. In general this simple scheme works well for the explanation of experimentally observed amphiphilic structures.

Accordingly, one very common method of self-assembly is the formation of amphiphilic bilayers, in which the hydrophilic polar heads of the amphiphile face the aqueous surroundings and the hydrophobic parts of the amphiphiles constitute the interior of the bilayers (figure 2). In the simplest arrangement, these bilayers just form planar structures. However, it is also possible that the bilayers close, thereby forming closed objects which are called vesicles, and that in the simplest case they have a spherical shape (figure 3). Of course, vesicles are not static in nature but typically highly dynamic systems where shape fluctuations may be pronounced and important for the understanding of some of their properties [8–10]. However, this will not be discussed in this article.

Such vesicles can structurally be subdivided into various classes. As a first case, they may just be comprised of one single bilayer (unilamellar vesicles). Here one can distinguish between small unilamellar vesicles (SUV; $R = 4$–20 nm) and large unilamellar vesicles (LUV; $R = 50$ nm–10 μm), where this distinction may be drawn on the basis of whether a molecule in the bilayer still experiences the fact that it is a curved bilayer (SUV) or where, on a molecular basis, the bilayer is effectively planar (LUV). Accordingly LUV are defined by $cL \ll 1$, where c is the curvature of the vesicle, i.e. the inverse of its radius, and L the maximum dimension

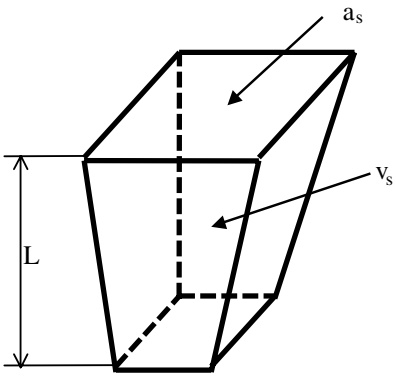

Figure 1. A schematic drawing of a surfactant molecule, showing the curvature packing parameter.

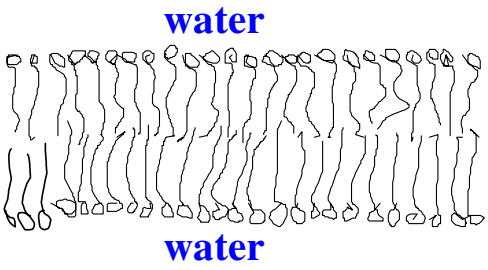

Figure 2. A schematic drawing of an amphiphilic bilayer.

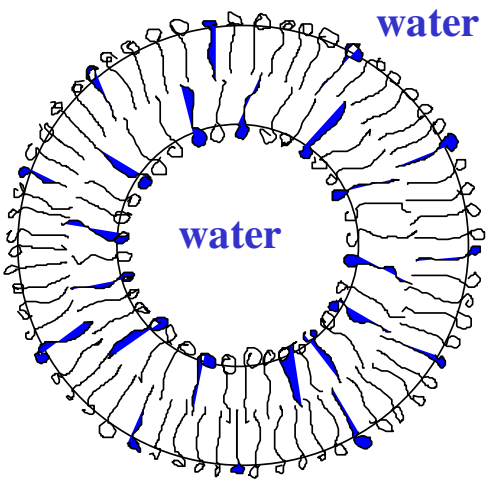

Figure 3. A schematic drawing of a vesicle.

of the amphiphilic molecule. Unilamellar vesicles form isotropic solutions (except for high concentrations, where gels may also be formed; see later) that are often denoted as L_4 phases.

In addition to the unilamellar case there exists also the possibility of multilamellar vesicles (MLV) [11] (for the case of phospholipids, often called liposomes [12, 13]) where one has various concentric shells of vesicles, i.e. a structure similar to that of an onion—why these phases are also sometimes called 'onion phases' [14].

As a general tendency, one finds that unilamellar vesicles are more likely to be observed for dilute systems, while MLV are frequently found in more concentrated surfactant systems. Typically, for bilayer-forming amphiphilic systems, one observes that with increasing concentration there exists a structural progression according to

$$\text{unilamellar vesicles} \rightarrow \text{multilamellar vesicles} \rightarrow \text{planar bilayers.}$$

For instance, such a tendency has been observed and studied in detail for the non-ionic surfactant cocodiethanolamide [15]. Typically, no macroscopic phase separation is observed for the transition from unilamellar vesicles to MLV or from MLV to planar bilayers. Instead, extended structurally biphasic, macroscopically homogeneous regions are observed that contain the different morphological structures in equilibrium, and that in general are relatively turbid.

In what situations does one observe vesicles? As a first requirement, the amphiphiles present have to have a propensity for the formation of bilayers. According to the geometric model, the formation of bilayers is to be expected if the packing parameter p is larger than $1/2$ [7, 16]. However, such a relatively large packing parameter requires amphiphiles with small head groups and bulky hydrophobic parts. Typically, this situation arises for double-chain hydrocarbon amphiphiles (e.g. normal phospholipids), perfluoro surfactants (as a CF_2 unit is much more space demanding than a CH_2 unit), or non-ionic single-chain surfactants with small hydrophilic groups (short EO chains; e.g. $C_{12}E_4$) [17]. Another way to increase the packing parameter of a surfactant system is by admixing a cosurfactant (e.g. a medium-chain alcohol). For many ionic surfactants such an admixture leads to the formation of bilayer structures [5, 18].

However, up to now we have not differentiated between the possibility that planar bilayers as in lamellar phases or even isotropic sponge phases [19–26] are formed instead of vesicles. Which are the parameters that determine whether vesicles or planar lamellae are formed? According to the packing considerations, planar bilayers should be formed if the packing parameter $p = 1$. However, for smaller values, vesicle formation may be preferred, as this reduces the energetically unfavourable edges of finite planar bilayers. Accordingly, one may expect vesicle formation for p-values not too close to 1 [7, 16, 27]. Another important quantity is the bending elasticity of the bilayer, i.e. the resistance it offers towards a deformation away from a preferred, spontaneous curvature c_0 of the bilayer. The bending properties are described by two elastic moduli, the mean bending modulus κ and the Gaussian modulus (or saddle-splay modulus) $\bar{\kappa}$. The free energy of bending of a bilayer system can be calculated by integration over the total surface of the bilayers according to [28]

$$F_b = \int \mathrm{d}A\, [(\kappa/2)(c_1 + c_2 - 2c_0)^2 + \bar{\kappa} c_1 c_2] \tag{2}$$

where c_1 and c_2 are the principal curvatures and c_0 the spontaneous curvature of the bilayer.

This integration can be performed straightforwardly in a simplified way for the various bilayer structures for the case of a vanishing spontaneous curvature ($c_0 = 0$). By comparison of the calculated energies, one can construct a simple phase diagram (figure 4) where the energetically favoured structure depends on the two moduli κ and $\bar{\kappa}$. For positive values of $\bar{\kappa}$, the isotropic sponge phase (L_3 phase) is the most stable, while for negative values of $\bar{\kappa}$, planar lamellae become more stable. In addition, one finds that if the Gaussian modulus $\bar{\kappa}$ becomes negative enough, a transition from planar bilayers to vesicles is to be expected even for a symmetric bilayer, i.e. one that has a spontaneous curvature of $c_0 = 0$ [29].

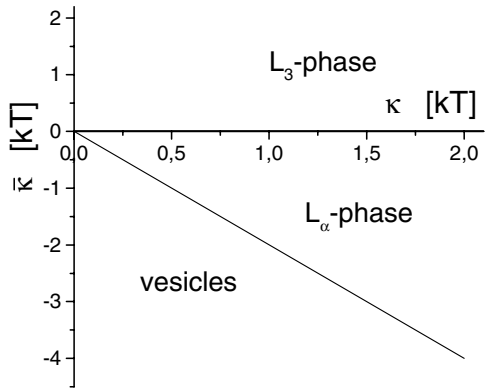

Figure 4. A schematic phase diagram for the different bilayer morphologies as a function of mean bending modulus κ and saddle-splay modulus $\bar{\kappa}$ for a system with a spontaneous curvature $c_0 = 0$ (according to [29]).

Vesicles are of interest not only from a fundamental point of view, as they are one of the principal structures in which amphiphiles can self-assemble, but also due to their high potential for applications. Such closed bilayers are a model system for cell membranes [30] and can be used to study the physical properties of amphiphilic bilayers [31]. Furthermore, vesicles are able to encapsulate active molecules and therefore can be used as drug delivery systems [32, 33]. A particular application of this sort that has attracted a lot of attention is the use of liposomes as non-viral carriers in gene therapy [34, 35]. Accordingly, they may be applied in a large variety of pharmaceutical and cosmetic [36, 37] applications.

This review is organized as follows. We will first give a brief overview of the various types of amphiphilic system that form vesicles and the conditions under which they are formed. Particular attention will be given to the spontaneous formation of vesicles, questions regarding their thermodynamic stability, and also the interesting fact that even extremely curved vesicles have been observed. In the second part we will concentrate on some aspects concerning the characterization of vesicle gels, i.e. densely packed systems of multilamellar or unilamellar vesicles that possess solid-like properties. In the last part we will discuss investigations of the dynamics of formation and breakdown of vesicles, as they can be studied by means of time-resolved experiments. Of particular interest in that context are the structures of intermediates formed during the transition process.

2. Vesicles

2.1. Formation processes for vesicles

A central point concerned with the observation of vesicles is the question of their preparation, as in many situations their formation requires the input of external energy. For instance, often vesicles are formed by the dispersion of lamellar bilayers where this dispersion may take place by dilution or by the input of external energy. In the following, we want to review briefly various methods by which vesicles can be formed. It should be noted that, of course, the size distribution of the vesicles formed is typically strongly affected by the method of preparation [15, 38].

In particular, for the formation of vesicles from relatively rigid bilayers (i.e. membranes with a large mean bending modulus κ), various methods have been advanced. Typical

representatives for amphiphiles that have such rigid bilayers are the phospholipids, which are the main amphiphiles forming the membranes of living cells.

A classical way of forming phospholipid vesicles is the by method of sonication of aqueous dispersions of the lipid [36, 39–41]. In some situations, vigorous shaking or vortexing will already be sufficient for the mechanical dispersion of the lipid [12, 13]. It should be noted that such treatment is a standard procedure for achieving homogenization of surfactant samples; i.e. in many situations where vesicles are observed experimentally their formation may be due to such homogenization of the samples.

Another classical method is thin-film hydration where a thin film of amphiphilic material is created by evaporation of a solution of amphiphile in chloroform or other volatile solvents. Afterwards this thin film comes into contact with water and dissolves by forming vesicles [13].

Another technique for vesicle preparation is the method of high-pressure extrusion of lamellar phases (or the microfluidization technique) [42, 43], where the shear forces tear the lamellar sheets apart and the fragments formed close to form surfactant vesicles. By the use of membrane filters of a given pore size, this method also allows for the formation of relatively monodisperse vesicles [43, 44]. For soft membranes (as they are present for bilayers formed by short-chain surfactants or systems rich in cosurfactant), simple shearing is sufficient to transform planar lamellae to MLV (cf 2.2.).

Typically vesicles are formed by surfactants, i.e. low-molecular-weight amphiphiles (such as phospholipids). However, similar structures may also be formed by large amphiphiles such as block copolymers [45–49]. Examples of such vesicles have for instance been observed for polystyrene (PS)-*b*-polyethylene oxide (PEO) [50] in water and polystyrene (PS)-*b*-polyacrylic acid (PAA) in solvent mixtures such as dioxane/THF/H_2O and DMF/THF/H_2O [51]. The formation of vesicles by amphiphilic block copolymers can be explained by taking into consideration the interfacial energy between the core and outside solution, the stretching of the core-forming blocks, and the repulsive interactions between corona chains [52, 53].

It might be added that not only are block copolymers able to form vesicles but also they can be formed by amphiphilic graft copolymers. An example has been given of a graft copolymer with a poly-*L*-lysine backbone with grafted polyethylene glycol (PEO) and palmitic acid. Upon sonication of an aqueous dispersion in the presence of cholesterol, unilamellar vesicles are formed where the size of the vesicles is controlled by the molecular weight of the copolymer [54].

It should also be mentioned that polymeric vesicles can be obtained from vesicles formed by polymerizable amphiphiles [55–59]. Interesting for applications are polymeric vesicles that can become depolymerized again upon change of the environmental conditions. This may be achieved for amphiphilic lipids that contain amino acid groups and that are polymerized through peptide bonds [60] and for cyclic α-alkoxy acrylates that can become hydrolysed again after polymerization [61]. Polymeric vesicles can also be synthesized from block copolymers as in the case of poly(2-methyloxazoline)-*b*-poly(dimethylsiloxane)-*b*-poly(2-methyloxazoline) with polymerizable end groups [62]. These vesicles are even able to reconstitute channel proteins in the vesicle membrane [63]. It is also possible to use vesicles as a template for polymerization. For instance, one may solubilize styrene in non-ionic vesicles. After polymerization of the styrene the surfactant can be removed by hydrolysis and the corresponding hollow polymer spheres are obtained [64, 65].

As an interesting special case it might be noted that recently vesicle formation has even been reported for a pentaphenyl-substituted fullerene potassium salt [66].

Structurally very similar to the unilamellar vesicles formed by amphiphilic molecules are hollow nanospheres made from polyelectrolytes. They are obtained by stepwise deposition of

oppositely charged polyelectrolytes on a spherical substrate particle. After subsequent removal of the substrate particle, hollow spheres of variable architecture are obtained [67].

Finally, it might be noted that formation of vesicles is by no means restricted to aqueous solutions but has been observed similarly in reverse systems, i.e. for oil continuous systems [68–71]. A particularly interesting case of vesicle formation in THF from mixtures of oppositely charged block ionomers (poly(1, 2-butadiene)-*b*-poly(caesium methacrylate) and polystyrene-*b*-poly(1-methyl-4-vinylpyridinium iodide)) has been reported recently. The oppositely charged blocks form the inner part of the vesicles, and the polystyrene the outer and the polybutadiene the inner part of the vesicle shell [72].

2.2. Shear-induced formation of vesicles

As mentioned above, in order to observe formation of vesicles from lamellar phases it is often necessary to have an external force acting on the planar lamellae. A very important external force of this kind is shear force and accordingly shear-induced transitions between planar bilayer structures and vesicles have been the subject of a large number of investigations.

In a pioneering study on the systems AOT/brine [73] and SDS/pentanol/dodecane/water [74] it has been shown that originally present planar lamellae become first oriented by the shear field for low shear rates, while for higher shear rates a transformation to MLV takes place. The dependence of the bilayer structure on the shear rate $\dot{\gamma}$ can be summarized in the form of an orientation diagram. Moreover, it has been observed that the size of the MLV scales with the inverse of the square root of the shear rate [73, 74]. A dynamic study of the transitions involved in the size change of the MLV by means of light scattering, polarization microscopy, and conductivity measurements has shown that the size change can occur in a continuous manner (for small changes of the shear rate) or in a discontinuous manner (for large changes of the shear rate) during which the MLV are completely destroyed [75].

The formation of MLV is always accompanied by a pronounced shear thickening where the viscosity rises significantly compared to that of the phase of planar bilayers [76–78]. This is due to the fact that planar bilayers can slide along each other without offering much flow resistance, while the MLV formed produce a relatively densely packed system of aggregates.

For a further increase of the shear rate—or if one already has MLV present prior to shear—shear-thinning behaviour is observed [79]. Such shear thinning would already be expected if the MLV behaved as hard spheres. Shear thinning of hard spheres (silica particles of 28–73 nm in cyclohexane, volume fraction of 0.4–0.5) exhibits a scaling law with the inverse of the square root of the shear rate [80]. For the apparent relative viscosity η_r the following empirical relation has been shown to describe adequately the experimental data for dispersed silica particles over a large shear rate range [81]:

$$\eta = \eta_\infty + \frac{C}{\dot{\gamma}}\left[1 - \exp\left(-\frac{\eta_0 - \eta_\infty}{C}\dot{\gamma}\right)\right] \tag{3}$$

where η_0 and η_∞ are the limiting values of the viscosity at low and high shear rates, respectively, and C is a constant that can be defined in terms of a critical shear rate $\dot{\gamma}_c$ at which the viscosity reaches a value of $\eta = 0.5(\eta_0 + \eta_\infty)$. Accordingly C can be written as

$$C = \frac{\eta_0 - \eta_\infty}{1.593\,62}\dot{\gamma}_c. \tag{4}$$

Typically, one observes over an extended range of shear rates a scaling law:

$$\eta \sim \dot{\gamma}^{-A}. \tag{5}$$

As stated above, the exponent A for hard spheres has been found experimentally to be about -0.5 over an extended range of shear rates [80]. A very similar shear-thinning behaviour has been observed for unilamellar phospholipid vesicles with radii of 250 nm [82].

However, the shear-thinning behaviour for MLV is actually even more pronounced; i.e. the exponent A is larger than 0.5, as it has been observed that the size of the MLV becomes smaller since bilayer shells become successively stripped off with increasing shear rate [83]. For the case of MLV in the system 90 mM TDMAO/10 mM TTABr/220 mM 1-hexanol, a value for A of 0.76 has been observed; i.e. it is much more pronounced than in the ideal hard-sphere case [77].

The transformation of planar lamellae to MLV does not necessarily depend on the shear rate, but in many situations it is controlled by the strain $\gamma = \dot{\gamma}t$ as has been shown for the AOT/brine system [84] where a critical strain for the onset of MLV formation could be defined from the shear-thickening behaviour and from small-angle light scattering typical for spherulites. For this system it could be shown that the shear stress controls both the MLV formation rate and their final size. Similar results have been observed for mixtures composed of alkyldimethylamine oxide and cosurfactants such as hexanol, heptanol, and octanol [85]. Apparently for the latter system a perpendicular orientation of the planar lamellae prior to the formation of vesicles is a necessary prerequisite, as has been observed in time-resolved SANS experiments. In SAXS experiments in a Couette cell on the lamellar phase of the system SDS/decanol/water, such a perpendicular orientation was preferentially observed at the inner wall, i.e. at the stationary inner cylinder of the shear cell [86].

It might be added that the shear-induced transition from L_3 phases to MLV has also been observed where, however, this transition was found to be reversible [87]. Finally, it might be mentioned that in some special situations it has also been observed that application of shear can induce a transition from vesicles to rod-like micelles [88, 89].

However, so far no consistent picture of a general description for the shear-induced transformations of lamellar systems has emerged and the details of these structural transitions depend subtly on the molecular composition and the concentration of a given system [90].

2.3. Spontaneous formation of vesicles

An important question regarding the stability of vesicles has already been addressed at the beginning, when we considered the process of formation of vesicles. In many circumstances, vesicles are only formed after the input of external energy. The conditions of formation are a very important point in themselves and also the question of thermodynamic stability of such vesicles arises naturally from the fact that in many situations they are not formed directly but require some external stimulus.

Therefore it should be emphasized that spontaneous formation of vesicles is a very important process, as here no such external driving force is required. However, it is by no means unambiguous how one defines the process of spontaneous vesicle formation, since in almost all circumstances for the preparation of samples it is necessary to apply some sort of shear to the system in order to homogenize it. Therefore it is always a key question whether this shear applied during homogenization may have been instrumental in the formation of observed vesicles—and whether they might not have been formed at all (or in a different morphology) without these shear forces.

One early observation of spontaneous vesicle formation was in the case of dialkyl dimethyl ammonium surfactants when halide counterions become replaced by hydroxide or acetate counterions [91, 92]. The reason for the different behaviour of the hydroxide surfactant and corresponding halide surfactants is that the hydroxide ion has a much higher affinity to water

and therefore resides on average further away from the charged micellar surface. Therefore the repulsive interaction between the head groups, and hence also the head group area, for the surfactant molecules at the amphiphilic interface becomes larger. Accordingly they do not form planar bilayers but have a tendency to form curved bilayers, i.e. vesicles. In these systems, even the size of the vesicles can be controlled by titration with an acid, which leads to growth of the observed vesicles [92, 93]. A similar strong dependence of the formation of vesicles on the counterion present has been observed for anionic surfactants. Here the exchange of the monovalent Na^+ of SDS with the divalent Ca^{2+} has been found to induce the formation of vesicular structures in mixtures with the zwitterionic TDMAO where the pronounced synergism in this system has been attributed to the strong binding of Ca^{2+} to the sulfate head groups, thereby effectively forming a double-chain surfactant [94].

Another case of spontaneous vesicle formation has been reported for aqueous solutions of fatty acids where vesicles are formed as a function of pH [95–97] by deprotonation of the fatty acid. Such a system can be regarded as an anionic carboxylate surfactant that contains the corresponding acid as a cosurfactant. An increasing content of the fatty acid reduces the head group area required per amphiphile. Correspondingly, the curvature of the aggregates formed becomes smaller until bilayers are formed. Oleic acid has also been employed as a cosurfactant together with a mixture of an amphoteric surfactant and an anionic surfactant, where for a given ratio of the two surfactants unilamellar vesicles are formed over an extended concentration range of 0.2–5 wt% surfactant [98].

Meanwhile, a classical situation for spontaneous formation of vesicles is that of catanionic systems, where vesicles are obtained by mixing a cationic and an anionic surfactant. For such 'catanionic' systems, vesicle formation has been observed for a large variety of different situations [99–106]. Most frequently, mixtures of anionic and cationic single-chain surfactants have been studied. Examples of such systems include SDS/DTAB [99], cetyltrimethylammonium tosylate (CTAT)/sodium dodecylbenzenesulfonate (SDBS) [100, 101], DTAB/SDBS [102], and CTAB/SOS [103]. For salt-free catanionic solutions, even the formation of regular hollow icosahedra has been observed [107].

Typically one observes for such mixtures that, for equimolar composition, precipitation takes place while, for an excess of either cationic or anionic surfactant, stable unilamellar vesicles are formed. The precipitate will often become transformed into a vesicle phase upon heating. In principle, the phase diagram should be symmetric about the axis of equimolarity where the extent of symmetry and the range of the vesicle phase depend strongly on the choice of cationic and anionic surfactant (figure 5). In general, it is observed that the more different the chain lengths of the two surfactants are, the more asymmetric the phase diagram will be and the more different the extensions of the vesicle phase on either side of the equimolarity line will be. The transition to micellar phases that border in the phase diagram on the vesicle phase can occur by means of a first-order transition, i.e. accompanied by a macroscopic phase transition, but also without such a phase transition. For instance, both types of transition have been observed in the catanionic system CTAB/SOS, depending on the total concentration of amphiphile [103].

However, there may also exist the possibility that no precipitate is formed for equimolar catanionic mixtures at room temperature. Such phase behaviour has been reported for alkyltriethylammonium bromide and sodium alkylsulfonate when the alkyl chains are octyl or decyl and also for longer chains of the cationic surfactant when mixed with octylsulfate [108]. Of course, the tendency for precipitation increases with the length of the alkyl chains and will be more pronounced for chains of similar length than for ones with large differences in length. In addition, the nature of the head group has a strong influence on the formation of precipitates, as for instance for the above-mentioned system: a replacement of the alkyltriethylammonium

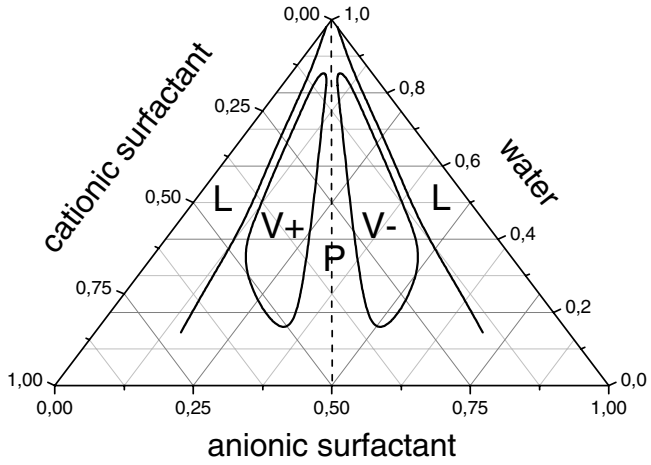

Figure 5. A schematic phase diagram of a mixture of a cationic and an anionic surfactant. L: micellar phase; P: precipitate; V+: positively charged vesicles; V −: negatively charged vesicles.

bromides by the corresponding alkyltrimethylammonium bromides or a replacement of the alkylsulfonates by the corresponding alkylsulfates leads to systems that form precipitates at room temperature. Evidently, the tendency for precipitate formation depends strongly on the ability to form a stable crystalline arrangement of the cationic and anionic surfactant molecules and this tendency may be suppressed by reducing the effective electrostatic interaction between the oppositely charged head groups, as is for instance the case for the bulkier triethylammonium head group.

However, vesicles are not only formed for catanionic mixtures of single-chain hydrocarbon surfactants; it is also possible that one [109] or both [110–112] of the chains may be a perfluoro chain. Another option is to have a mixture of a double-chain surfactant with a single-chain surfactant, such as has been studied for the case of didodecyldimethylammonium bromide (DDAB)/sodium dodecylsulfate (SDS) [113–115], or even two double-chain surfactants, e.g. as in the case of DDAB/sodium bis(2-ethylhexyl)sulfosuccinate (AOT) [116]. Then there exists also the possibility of using a gemini surfactant, e.g. a bis(hexadecyldimethyl ammonium) alkane, together with an oppositely charged single-chain surfactant [117]. The properties of various such catanionic systems have been summarized in a recent review [118]. Closely related to catanionic systems are mixtures of zwitterionic and anionic surfactants. In such mixtures, the zwitterionic surfactant can become partially protonated (either directly by the water or by some added acid) and then effectively form a catanionic mixture, which may lead to vesicle formation [119].

The extension of the vesicle phase in catanionic surfactant mixtures in general depends strongly on the type of the counterions present. An upper concentration limit for the presence of unilamellar vesicles will typically be reached once they start to be densely packed [79, 101]. Here the main factor will be the size of the vesicles that is controlled by the preferred curvature of the bilayers, but the effective packing density will also depend strongly on the intervesicle interactions. Since the dominating interaction in catanionic mixtures is of electrostatic nature, it is to be expected that the ionic strength and also the nature of the counterions will have a strong influence. Accordingly, it has been observed that a replacement of chloride ions by bromide ions in mixtures of dodecyltrimethylammonium halide and SDBS leads to an increase of more than a factor of two with respect to the existence range of the vesicles [120]. This

effect may be explained by the fact that bromide ions are more closely bound to the amphiphilic interface and thereby reduce the intervesicle electrostatic repulsion.

It might be added here that recently it has been shown that catanionic vesicles can also be employed as templates for the formation of hollow silica spheres. By acid-catalysed hydrolysis of tetramethoxysilane (TMOS), hollow silica particles with a 1–2 nm thick shell and with a core diameter identical to that of the templating vesicle are formed [121].

It should be noted here that mixing of conventional anionic and cationic surfactants leads not only to the formation of a catanionic surfactant pair but also to an equal amount of salt being formed by the corresponding counterions. This means that such systems possess a substantial ionic strength and typically are under conditions where the electrostatic interactions are effectively shielded.

However, it is also possible to have such systems under conditions without additional salt. This can be achieved by mixing the acid of the anionic surfactant with the hydroxide of the corresponding cationic surfactant; upon recombination, they form water. Such salt-free catanionic systems may exhibit a larger vesicle region in the phase diagram than their corresponding counterparts with added salt [107, 122].

Directly related to catanionic mixtures are systems where one of the ionic surfactants is replaced by a hydrophobic ion (that by itself does not form micelles, but in the mixture with an oppositely charged surfactant acts very similar to a correspondingly charged surfactant molecule). Such a situation is observed for mixtures of cetyltrimethylammonium bromide (CTAB) and sodium 3-hydroxy-2-naphthoate [123–125], or cetyltrimethylammonium 5-methyl salicylate [126]. A systematic study [127] on alkyltrimethylammonium 5-ethyl salicylate, where as alkyl chains dodecyl (C_{12}), tetradecyl (C_{14}), and hexadecyl (C_{16}) were employed, showed that for all these surfactants the first aggregate type formed by increasing concentration are LUV and not micelles as is typically the case for surfactants, i.e. instead of observing a cmc (critical micellar concentration), a cvc (critical vesicle concentration) is observed. Upon increasing the concentration, a transition from these LUV to large MLV takes place for C_{14} and C_{16}, while for the shorter chain C_{12} the formation of planar bilayers is observed. In the transition regime no two-phase separation is observed but it is accompanied by an increase in turbidity.

Studies on the system CTA (cetyltrimethylammonium)/HNC (3-hydroxynaphthalene-2-carboxylate) showed a behaviour similar to that observed for catanionic surfactant mixtures; i.e. with increasing HCN content first a low-viscosity solution, then a viscoelastic gel, and finally in the range of equimolarity a viscoelastic lamellar phase of densely packed MLV are found. For this system it has been noted that addition of salt (for instance the amount present from mixing two surfactants without using their hydroxide/acid version) changes both microstructure and macroscopic behaviour significantly; i.e. the salt-containing system at equimolar conditions contains vesicles but also stacked bilayers and tubuli. This results in much less pronounced elastic properties and there is no longer a yield stress [128]. Further investigations on the salt-free system (CTA/HNC) have shown that a vesicle $\rightarrow$ worm-like micelle transition can be induced in three different ways, i.e. by increase of temperature, by addition of a surfactant, and by shearing. This has been explained as being the result of a process of dissociation of the oppositely charged amphiphiles that leads to a 'surface melting' [129].

In a similar way it is possible to tune the aggregate shape systematically by changing the hydrophobicity of the counterion, as can for instance easily be done for the case of tetra-alkyl ammonium counterions. The bulkier the counterion, the less curved the aggregate shape. For instance for dilute solutions of perfluorodecanoate, it has been shown that replacing tetramethylammonium by butyltrimethylammonium or dibutyldimethylammonium leads to a transition from long rod-like micelles to unilamellar vesicles [130].

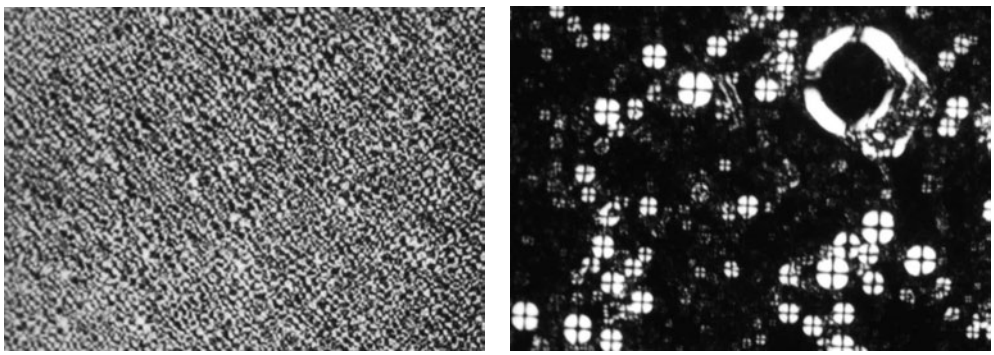

(a) (b)

Figure 6. Typical textures of phases containing MLV observed by means of polarizing light microscopy. (a) Woven (marbled) texture of a sample composed of 15 wt% SDS (sodium dodecyl sulfate), 7.5 wt% butanol, and 70 wt% decane in 7.5 wt% water (this is a case of a reverse MLV phase; (b) Maltese crosses that are typical for lamellar droplets (spherulites) in a sample composed of 8 wt% SDS, 15 wt% pentanol, and 38.5 wt% decane in water.

Vesicles are also observed in the diluted region of binary phase diagrams of non-ionic single-chain surfactants such as $C_{12}E_4$, where this phase has been denoted as L_α^+ [131, 132] and where the vesicle formation strongly depends on the temperature. Such vesicles can become stabilized by the addition of a stiff molecule such as cholesterol [133], by admixture of an ionic surfactant [134], or by addition of cosurfactant such as benzyl alcohol [76]. Similar phase behaviour has been observed for ethoxylated perfluorocarbon alcohols, which form unilamellar vesicles with radii of 100–400 nm in the dilute range of the phase diagram [135].

The presence of a cosurfactant (e.g. aliphatic alcohol or amine) has been reported to facilitate the formation of vesicles for a variety of different systems [17, 78, 112, 136–148]. However, it should be noted that almost all of these systems have a tendency to form large MLV which are very easily recognized by means of polarization microscopy where one observes typical textures for such systems that are either relatively homogeneous marbled textures (figure 6(a)) or Maltese crosses, as they are typical for spherulites (figure 6(b)) [15, 137, 149].

Vesicle formation can also be induced by the addition of amphiphiles with polymeric hydrophilic head groups, e.g. stearyl alcohol monoether with a PEO group of 5000 molecular weight, to a surfactant solution [150]. Such PEO-modified lipids can be employed to enhance the stability of phospholipid vesicles [151].

Spontaneous formation of unilamellar vesicles and MLV has also been observed for cationic siloxane surfactants after addition of salts with strongly binding counterions [152].

Another interesting system where spontaneous vesicle formation occurs is that of stiff rod-like amphiphiles that contain oligo(*p*-phenylene) as the hydrophobic block and an amine diethyl carboxylic acid head group. For such amphiphiles, vesicle formation has been observed for mixtures of these amphiphiles with octyl D-glucopyranoside after dialysis, where the glucopyranoside becomes removed [153, 154].

Finally, it should be added that spontaneous formation of vesicles is not restricted to aqueous systems, but has also been reported for mixtures of sucrose monoalkanoate and hexaethyleneglycol hexadecyl ether in decane [70] and for organic solvents with long-chained bisschiff bases and their organometallic complexes [155].

An interesting aspect of vesicle formation is the question of how the transition from micellar aggregates to vesicles takes place in the phase diagram, i.e. whether it constitutes a first-order phase transition or not. In most situations one observes a two-phase region by

which the micellar phase and vesicle phase are separated macroscopically. However, there exist also other situations, for instance that in catanionic mixtures of dodecyltrimethylammonium chloride (DTAC) and SDBS, where a continuous transition from micelles to unilamellar vesicles has been observed by means of dynamic light scattering, NMR self-diffusion and relaxation measurements, and time-resolved fluorescence quenching measurements [120].

An interesting approach that can be taken to check whether vesicle formation takes place spontaneously and to obtain information regarding the thermodynamic stability has been devised on the basis of *in situ* preparation of the corresponding surfactant systems. This can be achieved if one can start from a non-bilayer system and, by means of a chemical reaction, change its composition in such a way that it should form a bilayer structure. The advantage of this approach is that here this newly formed bilayer system can be produced without the application of shear forces; i.e. the bilayer structure is formed by purely diffusive processes.

An example of such an experiment is the aqueous solution of 100 mM TDMAO and 220 mM 1-hexanol, which forms an isotropic, low-viscosity L_3 phase (a sponge phase). If, to such an L_3 phase, an ester that hydrolyses easily is added, the acid formed will immediately protonate the zwitterionic TDMAO, thereby forming the cationic surfactant $TDMAOH^+$ according to

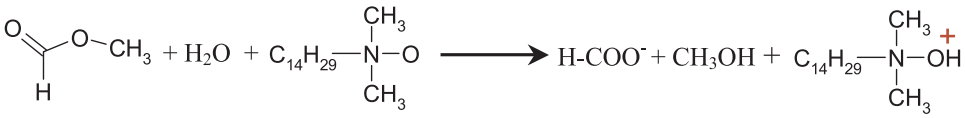

However, the presence of small amounts of $TDMAOH^+$ ($<1\%$ in the surfactant mixture) will already render the L_3 phase unstable and instead, in the conventionally prepared phase diagram, one finds a highly viscous phase of MLV. 'Conventionally prepared' means that the samples are prepared by weighing all the components into test tubes, mixing them vigorously, and letting them stand at a given temperature for some time.

If such a sample, that contains 10 mol% $TDMAOH^+$, is produced by addition and hydrolysis of 10 mM methyl formiate, a low-viscosity phase with strong birefringence and the typical texture of lamellar phases is observed. Electron microscopy could prove that this phase is composed of planar bilayers [156]. This reaction was followed by SANS experiments (figure 7) which show that the addition of the methyl formiate leaves the original L_3 structure intact. However, as the hydrolysis proceeds, a pronounced correlation peak of the lamellar phase develops that becomes sharper with time; i.e. the lamellar phase becomes more highly ordered. After vigorous shaking of the sample, the correlation peak is much broader again. At the same time, shaking changes the originally low-viscosity sample to a gel-like sample with a shear modulus G_0 of about 15 Pa (as would have been observed by the conventional preparation method). Freeze-fracture electron microscopy shows that this shaken sample now contains polydisperse MLV with diameters of 0.5–2 μm [156].

Evidently, in this system, both bilayer structures, i.e. planar bilayers and MLV, are long-time stable, as it has been verified that both structures are retained for several months without noticeable change. In fact, the situation is even more complicated, as this system may further be exposed to shear. If very high shear rates are applied ($\sim$5000 s^{-1}) for some time ($\sim$1 h), the originally present large MLV not only become smaller, but also they are finally transformed into SUV of 100–200 nm diameter [157]. However, even this third state has been shown to be long-time stable after cessation of shear; i.e. one has the situation where for a given sample composition, planar lamellae, MLV, and SUV are stable structures. In this case, so far there has not been the possibility of determining which of these different structural states is the thermodynamically stable state, and it serves as an example that the structure of vesicles may strongly depend on the history, in particular the shear history, of an amphiphilic system.

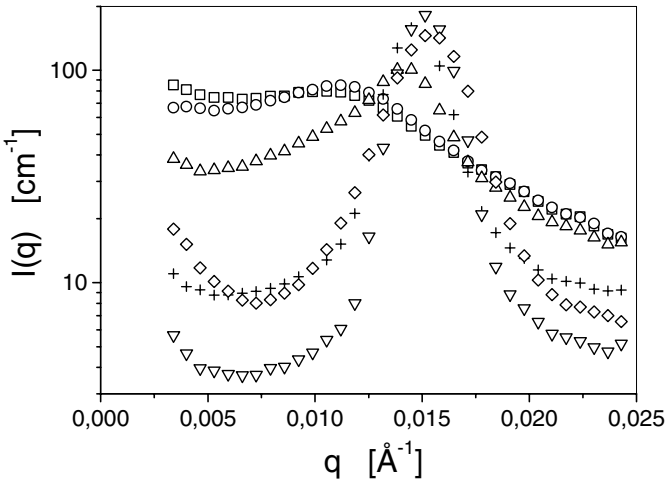

Figure 7. The radially averaged SANS intensity as a function of the scattering vector q for the system 100 mM TDMAO/220 mM 1-hexanol in D_2O before and after addition of 10 mM methyl formiate. □: original L_3 phase; ○: directly after addition of the methyl formiate; △: after 25 min; +: after 65 min; ▽: after 28 h; ◇: after shaking.

A similar situation has been encountered for mixtures of zwitterionic TDMAO and anionic sodium dodecyloligoethoxysulfate. If that system becomes protonated by hydrolysis of methyl formiate, a catanionic surfactant pair is formed. However, by the chemical reaction, planar bilayers are formed that are transformed into vesicles only by applying shear forces [158]. A similar result has been observed for the catanionic system tetradecyltrimethyl ammonium (TTA)/laurate. Without shear forces, planar lamellae are formed when a hydrolysis reaction is employed for the preparation and after shearing MLV are present [159]. Accordingly, it may be the case that for a number of catanionic surfactant systems where spontaneous vesicle formation has been reported, vesicles were actually only formed due to shear forces that are present during the homogenization process.

However, it should be mentioned that the preparation by means of chemical reaction does not exclude the possibility of forming vesicles by purely diffusive processes. This has been demonstrated for mixtures of TDMAO/NaHNC (3-hydroxynaphthalene-2-carboxylate)/formic acid/water where vesicle formation is not only observed for conventionally prepared samples but also when the phases are formed by a hydrolysis reaction of methyl formiate [160].

Finally, it should be stated that there exist numerous situations where spontaneous vesicle formation has been reported and this article will certainly not give complete coverage of all the various systems that have been studied.

2.4. Thermodynamic stability

Of course, the fact that 'spontaneous' vesicle formation takes place for a variety of surfactant systems does not necessarily mean that in all these cases thermodynamically stable vesicles are formed. In fact, the question of thermodynamic stability is still a controversial issue [161], but meanwhile there exists evidence that at least in some situations vesicles might be a true equilibrium state. In almost all of the cases mentioned above, homogenization of the samples is necessary, and this implies that these samples were subject to shear forces, although sometimes only to a minor extent. Therefore it is interesting to consider further evidence from other

experiments that addresses in more detail the question of thermodynamic stability of the vesicles investigated.

A very interesting observation has been reported for the binary surfactant system of the ganglioside GM3 where spontaneous formation of SUV (diameter: ≈50 nm) can be induced reversibly by a temperature change [162–164]. More recently, thermoreversible formation of MLV has also been observed which takes place around room temperature upon heating a microemulsion of tetradecyldimethylamine oxide with hexylacetate [165].

A similar thermoreversible formation of vesicles was found for copolymer vesicles of PS-*b*-PAA in various polar solvent mixtures. Here, not only are the vesicles formed thermoreversibly, but also their size is well controlled by either the temperature or by the solvent composition [51]. With solvent mixtures of dioxane/THF/H_2O or DMF/THF/H_2O it has even been observed that the vesicle size can be changed reversibly by changing the solvent composition; i.e. for increasing water content, an increase of the vesicle size is observed [166]. In this apparently thermodynamically stable vesicle system, increasing water content increases the interfacial energy and accordingly the interfacial area is reduced, which leads to an increase of the vesicle size. For this system it was found that large vesicle sizes correspond to a wide size distribution, whereas for small vesicles a narrow size distribution is observed [51].

Another case of reversibly formed vesicles has been reported for solutions of oleyldimethylamine oxide (ODMAO) at intermediate concentrations of 50–150 mM. In this system vesicles are formed when about 50% of the ODMAO have been protonated by a strong acid (HCl). For this system, reversible vesicle formation/dissolution has been observed upon changing the pH [167].

In general, a reversible formation/breakdown process for vesicles is a strong indication for thermodynamical stability.

2.5. Theoretical explanation of spontaneous formation of vesicles

The explanation of spontaneous vesicle formation on a theoretical basis is not yet completely established and still a topic of ongoing research. The description of multilamellar systems is difficult and so far it is mainly the unilamellar case that has been analysed in detail.

The most analysed and best-understood case is that of vesicles formed by mixed surfactants. On the basis of the curvature elasticity of the amphiphilic bilayer, it can be shown that an energetic stabilization of vesicles is possible. A first analysis in terms of the bending moduli was performed by Helfrich [168] and there, already, a size distribution for the vesicle radii was derived according to which the distribution function is given by

$$f(R) = \frac{8R^3}{\langle R^2\rangle^2}\exp(-2R^2/\langle R^2\rangle) \tag{6}$$

where $\langle R^2\rangle$ is the mean square radius. Later extensions of this analysis that in addition apply a multiple equilibrium analysis of this problem have shown that the pre-exponential factor in equation (6) depends strongly on the assumptions that are used in the calculations while the exponential term is principally retained [79, 169, 170].

For the case of catanionic surfactant mixtures, it has been shown that, depending on the interactions between the two different amphiphiles, the composition between the inner and outer monolayers that compose the bilayer will differ, and this asymmetric composition will lead to an effective spontaneous curvature of the bilayers, where the effective spontaneous curvatures of the inner and outer layers are of equal and opposite signs. This mechanism predicts energetically stabilized vesicles [171, 172].

Extensions of the bending energy approach were applied to make model calculations for mixed sodium dodecyl sulfate (SDS)/dodecylammonium chloride vesicles. These calculations

showed a steep increase of the bending energy on approaching high mole fractions for either of the two surfactants and also for the equimolar situation. However, in the vicinity of the equimolar ratio a minimum for the bending free energy is observed which allows vesicle formation, which is in good agreement with the experimentally observed situation [173]. A more recent analysis based on the same approach showed that the effective bilayer bending modulus is lowered by surfactant mixing and this reduction is more pronounced when the charged surfactant has the larger head group and the smaller hydrophobic part [174].

An alternative way to describe the stability of two-component catanionic vesicles is based on a molecular thermodynamic model that takes into account the surfactant tail packing free energy (that accounts for the conformations of the surfactant tails in the hydrophobic region of the vesicle), surfactant head steric repulsions, and the electrostatic interactions. In this theory the total free energy of vesiculation is obtained as the sum of the standard free energy, the free energy of mixing (that accounts for the configurational entropy gain due to the mixing of the aggregates, the monomers, and the water molecules), and the interaction free energy (between aggregates and between the monomers) [175]. Of course, such a model yields also an asymmetric distribution of the various amphiphiles between the inner and the outer layer of the vesicle shell. On the basis of the molecular structure of the surfactant molecules, this theory then allows the prediction of vesicle size and composition distribution, surface charge densities, surface potentials, and the composition of the individual vesicle monolayers [175].

This theory has been used to study the effect of the difference in chain lengths of anionic and cationic surfactants on the vesicle formation. For a difference in chain length of the anionic and cationic surfactant that is not too large, vesicles are predicted that are entropically stabilized and possess a relatively broad size distribution [175]. If the asymmetry in the length of the alkyl chains of the surfactants becomes larger, it is predicted that the vesicles formed will be stabilized energetically. Such vesicles should be much smaller and possess a narrow size distribution [176].

More recent investigations indicate that unilamellar vesicles are stabilized by one of two distinct mechanisms that differ depending on the value of the bending moduli [177]. When the mean bending modulus κ is significantly larger than kT ($\kappa \gg kT$), the unilamellar vesicles are stabilized by the spontaneous curvature c_0. Such vesicles are energetically stabilized and will possess a low degree of polydispersity. An example of such a system has been given for the case of catanionic mixtures of CTAB with sodium perfluoro-octanoate [177]. Bilayers with lower bending moduli ($\kappa \approx kT$) form vesicles that are stabilized by Helfrich-type repulsive undulation forces and form much more polydisperse vesicles.

The case of the presence of both unilamellar vesicles and MLV has been discussed taking into account the bending energy and the entropic contribution [178]. Within this model the free energy of unilamellar vesicles and MLV as well as that of the corresponding planar lamellae was calculated for some typical values of the bending constants, i.e. for $\bar{\kappa}$ negative (-2–$5\,kT$) and κ large enough that the sum $2\kappa + \bar{\kappa}$ is in the region of kT. With these calculations a phase diagram can be constructed according to which low-concentration unilamellar vesicles are predicted, that become transformed into MLV with increasing concentration, and finally for still higher concentration a lamellar phase is formed [178]. This is in good agreement with experimental observation. The number of shells of the MLV is predicted to increase with increasing concentration and it is interesting to note that according to this model the multilamellar phase would be thermodynamically stable. This work also predicts that with decreasing κ the strength of the phase transition from small onion-like vesicles to large spherulites or the lamellar phase becomes weaker.

Experimentally it has been observed that the density of MLV increases upon approaching the L_1 phase in the phase diagram and decreases upon approaching the L_3 phase, and that these

vesicles possess an exponential size distribution [179]. This behaviour could be explained by a model based on the bending energy [179] and in general it has been argued that such multilamellar structures are stabilized by their positive Gaussian curvature [180].

Finally, it might be mentioned that even for tubular vesicles, as observed experimentally for aqueous solutions of dimyristoylphosphatidylcholine/geraniol [181], thermodynamic stability has been predicted by a bending energy model. However, for that purpose, fourth-order stabilizing has to be taken into account [182].

2.6. Ultrasmall unilamellar vesicles (USUV)

A very interesting point as regards the large variety of different vesicle structures and sizes is the existence of ultrasmall unilamellar vesicles (USUV). Such extremely small vesicles with highly curved bilayers have only been reported recently and here one encounters vesicle radii of 5–10 nm, i.e. here one has bilayers that are strongly curved even on a molecular length scale. Such USUV have been observed for:

- triton X-100/cetyl pyridinium chloride (CPyCl)/1-octanol [183, 184];
- ethenediyl-1, 2-bis(dodecyldimethylammonium bromide) [185];
- 2-O lauroyl saccharose/didodecyl dimethyl ammonium bromide (DDAB) [186];
- SDS/DDAB [114, 187];
- tetradecyl dimethyl amine oxide (TDMAO)/HCl/hexanol for a molar content of 40% of HCl with respect to TDMAO [188].

In all cases one finds that they are formed by ionic surfactants or for mixtures of ionic and non-ionic surfactants, i.e. for substantially charged amphiphilic interfaces, and only for relatively dilute solutions, i.e. typically for volume fractions of less than 3%. For instance, for the TDMAO/HCl/hexanol system they are only observed for an addition of 30–50 mol% of HCl to TDMAO (where the weak base TDMAO becomes protonated and is transformed to the cationic surfactant $TDMAOH^+Cl^-$) and for a total amphiphile concentration of less than 4 wt% [188]. Evidently strong electrostatic interactions and dilution are a necessary prerequisite for the formation of these strongly curved vesicles. This is corroborated by the observation that they readily disappear upon the addition of salt, i.e. on shielding the electrostatic interaction [188, 189]. For instance, for the TDMAO/HCl system, the presence of just 5 mM NaCl already prevents the formation of the USUV and instead large MLV are observed [188]. This means that on shielding the electrostatic interaction, strongly curved bilayers are destabilized.

Another interesting aspect is the fact that the USUV phase (denoted as L_4) is continuously connected with the conventional micellar phase (L_1) and is observed for higher cosurfactant contents; i.e. a transition from worm-like micelles to the vesicles takes place without a macroscopic phase separation [184, 188]. In figure 8 a cut through the phase diagram of TDMAO/HCl/hexanol is given for a constant molar mixing ratio of $TDMAOH^+/TDMAO = 1{:}1.5$. One observes that only for a relatively low surfactant concentration of less than 110 mM are vesicles (L_4 phase) formed, while the conventional micellar phase (L_1 phase) extends to much higher concentrations. The transition from micelles to USUV is induced by the addition of hexanol. At low hexanol concentrations a micellar phase of spherical micelles is present. Upon addition of hexanol, rod-like micelles grow until at 45–60 mM 1-hexanol a region is reached where rod-like micelles and ultrasmall vesicles are present in equilibrium without macroscopic phase separation. At still higher hexanol concentration, only the small vesicles (USUV) are observed. Upon further addition of hexanol, the USUV become unstable again and large MLV are formed in a macroscopically biphasic system of an isotropic solution which is

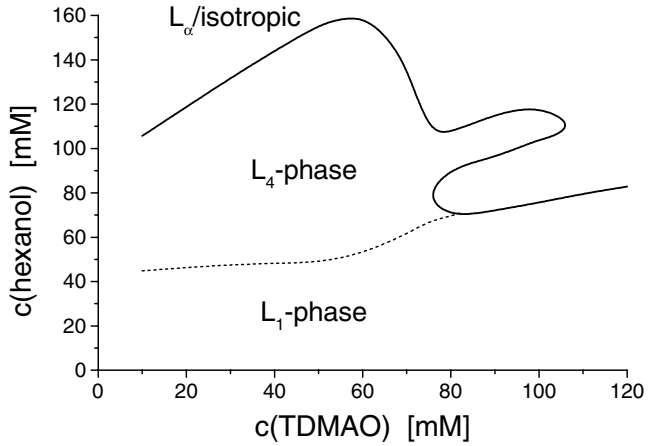

Figure 8. A cut through the phase diagram of the quaternary system TDMAO/HCl/1-hexanol/water at 25 °C; the surfactant and cosurfactant concentrations were varied. The degree of charging was kept constant at 40%; i.e. $c(\mathrm{HCl}) = 0.4c(\mathrm{TDMAO})$ [188].

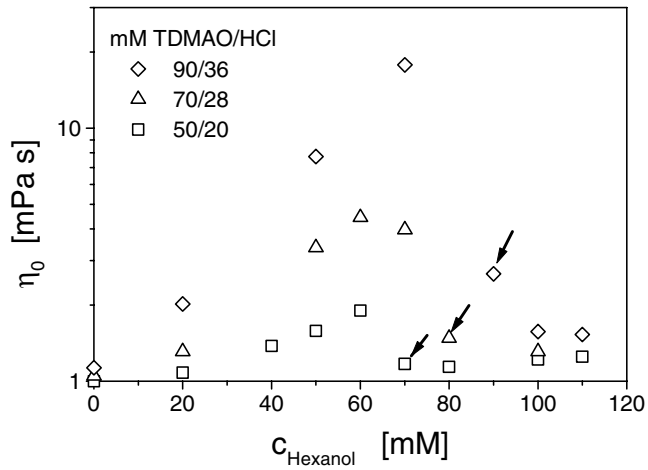

Figure 9. The zero-shear viscosity η_0 against the hexanol concentration. The degree of charging (HCl content relative to TDMAO) was kept constant at 40%. The TDMAO concentration was varied between 50 and 90 mM (the beginning of the L_4 phase is marked with an arrow).

in equilibrium with a birefringent MLV phase. This transition from USUV with a high bilayer curvature to the almost flat bilayers in the MLV can be explained by the fact that addition of hexanol leads to an increase of the packing parameter and beyond a certain content formation of planar bilayers will always be favoured.

Addition of hexanol to samples containing more than 110 mM surfactant does not lead to the formation of USUV; instead large MLV are always formed and one enters a biphasic region with macroscopic phase separation. Evidently the increase of the repulsive interactions between the charged USUV with increasing concentration renders them less stable compared to a multilamellar system.

The transition from rod-like micelles to USUV is not accompanied by a macroscopic phase separation. The experimental evidence from electric conductivity, viscosity, and small-

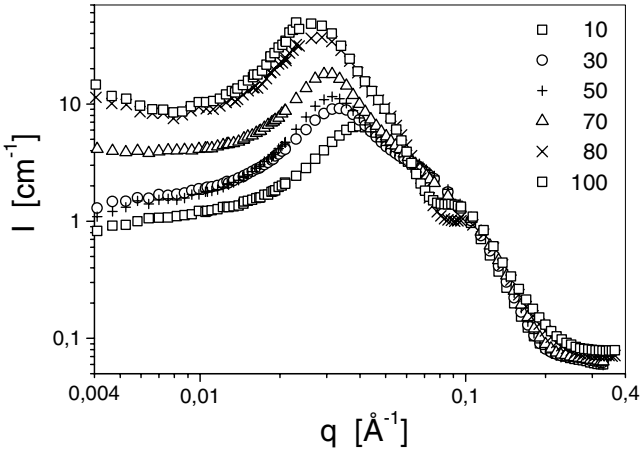

Figure 10. The radially averaged SANS intensity as a function of the scattering vector q for a series of samples containing 70 mM TDMAO/28 mM HCl and various concentrations of 1-hexanol at 25 °C. The hexanol concentration of the samples in mM is given in the inset.

angle neutron scattering (SANS) measurements [188] shows that this transition takes place continuously and in a very narrow intermediate-concentration range both different structures are present. This can be very nicely demonstrated if one looks at the zero-shear viscosity η_0 of such samples of given surfactant concentration for various amounts of added hexanol (figure 9). Initially the addition of hexanol leads to a pronounced increase of the viscosity, which can be attributed to the growth of rod-like micelles that are becoming entangled and thereby increase the viscosity. However, for further increase of the hexanol concentration a sudden drop of the viscosity takes place to values slightly higher than 1 mPa s, i.e. water viscosity. Here the rod-like micelles have been transformed into USUV and these small spherical objects in these solutions only have an effective volume fraction of 10–20% and increase the viscosity in a way similar to a hard-sphere dispersion, i.e. for this concentration, by less than a factor of 2 compared to the solvent viscosity.

This interpretation has been corroborated by SANS experiments (figure 10) which show a micellar correlation peak for low hexanol content which moves to lower q-values with increasing hexanol concentration, thereby indicating the micellar growth. An analysis of the scattering curves clearly shows that here rod-like micelles with a radius of 18–20 Å are present. The formation of the USUV is indicated by a newly appearing minimum around 0.08–0.09 $Å^{-1}$, which is characteristic for the vesicle size (as the vesicle radius is given by $R_{ves} = \pi/q_{min}$) and furthermore demonstrates that the vesicles formed have to be relatively monodisperse, i.e. they have a polydispersity index of 0.26–0.29. This value is in perfect agreement with a theoretically predicted value of 0.283 for fully equilibrated surfactant vesicles at high dilution [170]. In addition an analysis of the higher-q part of the scattering curves shows that here a bilayer structure must be present. The bilayer thickness is 22–22.5 Å and does not change markedly within the L_4 phase.

Of course, an interesting question is that of by which mechanisms such extremely curved bilayers are stabilized. A theory for their stability has been advanced that is based on the bending elasticity of the bilayers and calculates the electrostatic contribution to the bending moduli κ and $\bar{\kappa}$ by means of a numerical integration of the Poisson–Boltzmann equation. In this model a different concentration of the counterions inside and outside the vesicles is allowed for, and it is able to describe the size distribution of the vesicles as a function of the electrostatic

parameters, i.e. the number of charged surfactant molecules, total concentration, and salinity, and the intrinsic value for $2\kappa + \bar{\kappa}$, i.e. the value of the bare bilayer without the electrostatic contributions [189, 190]. Under certain conditions this model also predicts a transition from USUV to larger unilamellar vesicles [190].

3. Vesicle gels

At the beginning of this section we want to mention that the term gel phase in the context of bilayer phases is often employed for phases in which the alkyl chains of the amphiphile are in a crystalline state. Such a situation is often encountered for phospholipids around or somewhat below room temperature [191] and is similarly observed for corresponding synthetic surfactants such as dimethyl dioctadecyl ammonium bromide [192] and other double-chain surfactants [193]. Such bilayer phases may contain vesicular structures which can be unilamellar [194] or multilamellar [195–197] but they will not be addressed in this review; instead we will concentrate on phases in which the alkyl chains are present in a fluid state.

Dispersed vesicles yield low-viscosity solutions as long as their effective volume fraction (given by the volume fraction of the bilayer material and the encapsulated solvent) remains well below that of densely packed spheres. Once an effective volume fraction of 0.494 is reached, a hard-sphere crystallization would be expected to begin [198]. Of course, in general, vesicles are not really good examples of hard spheres but, nonetheless, one may expect that upon approaching dense packing the viscosity will increase strongly and will diverge for a further increase of the packing fraction; i.e. from a rheological point a solid-like system—a gel—is formed.

The formation of a vesicle gel depends on the size and concentration of the vesicles. By the name 'gel' we simply want to denote a surfactant system that possesses a yield stress; i.e. we use a simple rheological definition of a gel according to its macroscopic flow behaviour. A system that has a yield stress does not flow until an applied stress exceeds a critical value, i.e. the yield stress. In practice this means that such samples often do not flow under their own weight and will entrap air bubbles. It might be noted here that surfactants can form gels in various different ways that can differ substantially in their structure, and vesicle gels are just one subclass of such surfactant gels [199]. Other surfactant systems that exhibit gel-like properties include liquid crystalline phases, such as hexagonal phases, reverse hexagonal phases, and cubic phases [3, 200–202]. Networks of entangled rod-like micelles often exhibit strongly viscoelastic properties and appear to be gel-like. Contrary to our above definition, they possess no yield stress. However, in some circumstances their relaxation times may be very long and for such situations it can become difficult to distinguish between systems with a yield stress and those having none (as, of course, in general a definition of yield stress will always depend on the timescale chosen). Then, of course, there also exist a large variety of organogels where low-molecular-weight amphiphiles are employed to gel oily liquids [203–208].

The origin of the rheological properties of vesicle gels is particularly simple from a theoretical point of view: they result primarily from steric interaction between spherical objects and depend much less on specific molecular interactions, which are often important for other gel structures. A key parameter is the effective volume fraction of the vesicles, since for gel formation of spherical objects dense packing is required. However, the rheological properties of the vesicle system, such as the elastic or shear modulus (as well as the yield stress), not only depend on the dense packing but will also strongly depend on the strength of interaction between the vesicles, e.g. on the electrostatic interactions between the vesicles.

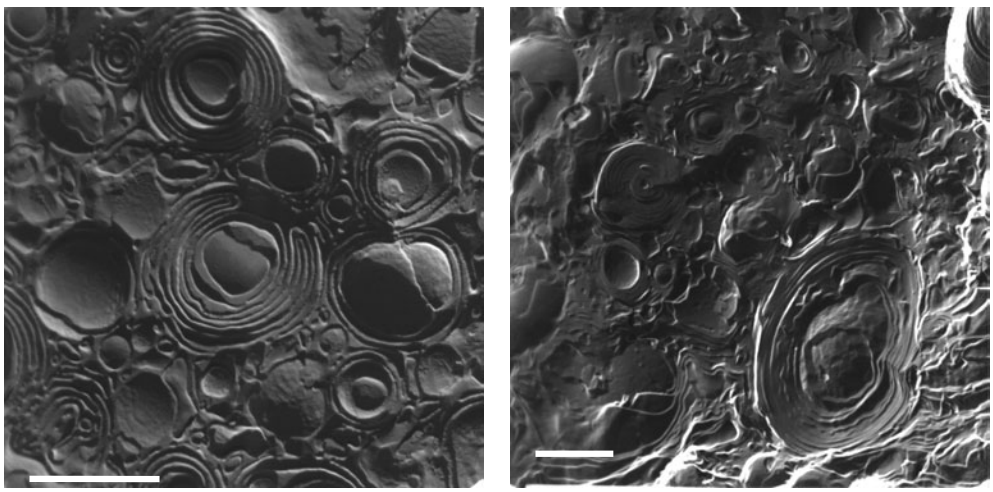

(a) (b)

Figure 11. Freeze-fracture electron micrographs of MLV in the system 90 mM TDMAO/10 mM TTABr that contain 201 (a) or 310 (b) mM 1-hexanol. The bars represent 1 μm.

3.1. Vesicle gels formed by multilamellar vesicles (MLV)

Very often a gel-like appearance of vesicles is found in a concentration range of 2–20 vol% when MLV are present. For instance, such vesicle gels are observed in systems based on non-ionic surfactants (such as alkylamine oxides) to which a medium-chain alcohol, as cosurfactant, is added. On increasing the concentration of cosurfactant, the original micellar surfactant solution is transformed into a lamellar phase, and for still higher concentration of the cosurfactant, an isotropic L_3 phase is formed [140]. In such systems it has been found that the microstructure of the lamellar phase depends strongly on the concentration of the cosurfactant. For low amounts of alcohol, MLV are formed, while for higher concentrations, planar lamellae are present. The vesicle phase already exhibits pronounced viscoelastic properties and a yield stress for concentrations of just 50–100 mM surfactant. One characteristic feature of such systems is a strong stress-induced birefringence that may for instance be observed when tilted samples are viewed between crossed polarizers [209].

The tendency of formation of MLV is strongly enhanced if the amphiphiles are not uncharged but contain ionic surfactants. For such charged systems the formation of planar lamellae may be completely suppressed and instead only vesicles are formed. Here it is interesting to note that this transformation can already be achieved by substituting for small amounts of 0.5–1 mol% of the uncharged surfactant (e.g. TDMAO) with an ionic surfactant (e.g. TTABr) [146]. Nonetheless, it is observed that the structure of the vesicles still depends strongly on the concentration of the cosurfactant. In the electron micrographs of figure 11 we see very round and well-formed vesicles for low hexanol concentration, while for higher hexanol concentration the vesicles are evidently much less well defined and assume various shapes that deviate strongly from sphericity. It appears that the increased cosurfactant concentration reduces the rigidity of the bilayers and the more flexible bilayers can assume more flexible shapes.

For more concentrated systems the normally spherical MLV may become deformed to polyhedral objects in order to achieve better space filling, as may be seen in the system TDMAO/TTABr/hexanol when increasing the surfactant concentration from 100 to 400 mM.

Figure 12. A freeze-fracture electron micrograph of a vesicle phase for a sample of composition 360 mM TDMAO/40 mM TTABr/780 mM 1-hexanol/700 mM NaCl in a H_2O/glycerol mixture that contains 20 wt% glycerol. The bar represents 2 μm.

Electron microscopy (figure 12) shows that here large polyhedral objects with diameters of 2–4 μm are present which contain densely packed bilayers; i.e. one such vesicle is made up from more 100 concentric bilayer shells. Deviations from spherical shape are more pronounced for larger packing density, i.e. concentration, of the bilayer system.

The tendency to form vesicles instead of planar bilayers upon charging of the bilayers can be explained in simple theoretical terms. Calculations of the electrostatic contribution to the bending moduli of bilayers have shown that an increasing charge density of the bilayer leads to an increase the mean bending modulus κ, while the saddle-splay modulus $\bar{\kappa}$ becomes more strongly negative [210, 211]. However, according to the phase diagram given in figure 4, such a decrease of $\bar{\kappa}$ will induce a transition from planar lamellae to vesicles.

Of course, the rheological properties of the MLV phase are very different from those of the planar lamellar phase. Typically, the storage modulus G' and the loss modulus G'' remain relatively constant as a function of frequency and G' is larger than G''; i.e. in such samples the elastic properties dominate over the viscous properties—i.e. they behave as Bingham fluids. Typical values for the shear modulus G_0 (the plateau value of the storage modulus G') for such gels of MLV are in the range of 1–100 Pa and they are similar even for systems that differ substantially in their molecular composition [14, 15, 158, 209, 213, 214].

In a simple first-order approximation one can state that the shear modulus G_0 of a vesicle gel should be proportional to the number density ${}^1N$ of the vesicles according to

$$G_0 = \chi {}^1NkT \tag{7}$$

where χ is a system-dependent parameter that accounts for the details of the packing, the number of shells, and the interaction potential between the vesicles [209, 215, 216]. Effectively, this corresponds to a description where during deformation an amount of energy of χkT per vesicle is stored elastically.

The rheological behaviour of vesicle gels is often such that they can be regarded as solid-like, and then the shear modulus G_0 can be related to the compression modulus K via

$$G_0 = 1.5K\frac{1-2\mu}{1+\mu} \tag{8}$$

where μ is the Poisson number (that has the limiting value of 0.5 for an incompressible system).

Another parameter that is reflected in the rheological properties of a vesicle gel is the stiffness of the bilayers that form the vesicles. The stiffness can be described in terms of the bending energy of the bilayers according to equation (2) [28], where the free energy is

determined by κ (the mean bending modulus), $\bar{\kappa}$ (the Gaussian (or saddle-splay) modulus), and c_0 (the spontaneous curvature).

If one considers the deformation of a vesicle with interlamellar spacing D, one can describe that situation by means of an effective surface tension σ_{eff} [217] which depends on the compression modulus B and an elastic modulus K (defined as κ/D) according to

$$\sigma_{eff} = 0.5\sqrt{BK}. \tag{9}$$

If one identifies the restoring force with the force that is due to the deformation of a vesicle and relates that to the Laplace pressure, one obtains for the shear modulus

$$G_0 = \frac{2\sigma_{eff}}{r} = \frac{\sqrt{nB\kappa}}{r^{1.5}} \tag{10}$$

where n is the number of shells of the MLV (defined by R_0/D, where R_0 is the vesicle radius).

In general, the layer compressional modulus B can be written as [218]

$$B = D^2\left(\frac{\partial^2(f)}{\partial D^2}\right)_n \tag{11a}$$

where n is the number of layers per unit length and f the free energy per unit volume.

According to Dubois *et al* [219], the compression modulus B corresponds to the osmotic pressure Π between the lamellae, i.e. is given by the thermodynamic equation of state of the amphiphilic system:

$$B = \Pi = {}^1N_i kT \tag{11b}$$

where ${}^1N_i$ is the number density of ions at the mid-plane between the bilayers.

Accordingly, gel formation depends on the strength of interaction between the vesicles that is given by the volume fraction, but the moduli B and κ depend also on the electrostatic conditions. In particular, the compression modulus B will strongly increase with increasing charge density of the bilayers. This has been observed experimentally for MLV of an initially uncharged amphiphilic system of TDMAO and hexanol into which increasing amounts of ionic surfactant were admixed. This results in a pronounced increase of the shear modulus until, at a degree of ionic substitution of ~5–7 mol%, a plateau value of the shear modulus was reached [209]. This is reasonable, as it has been observed by other experiments that in this range of 5–10 mol% ionic surfactant in an amphiphilic layer the electrostatic potential will become high enough to affect counterion condensation; i.e. a further increase of the content of ionic surfactant does not lead to stronger electrostatic interactions, as the additional charges will be shielded by the corresponding counterions. In the same study it was also observed that the shear modulus becomes reduced again if the electrostatic interaction is shielded by added salt [209].

Vesicle gels of densely packed MLV have also been observed for highly concentrated systems of 20–25 wt% TDMAO, 4–6 wt% of various cosurfactants such as benzyl alcohol or cyclohexanol, and in addition ~20 wt% hydrocarbon. In these systems, densely packed polydisperse polyhedral vesicles of 0.5–2 μm diameter are observed [220].

3.2. Vesicle gels formed by small unilamellar vesicles (SUV)

A particularly interesting situation arises when a vesicle gel is not formed by relatively polydisperse MLV but is instead built from well-defined unilamellar vesicles.

Such a system was first described in the literature a long time ago for the K oleate/decanol/water system [221]. Here, for a composition of 15 wt% K oleate/23 wt% decanol, a stiff, clear, and isotropic gel phase was observed that is very sensitive to changes

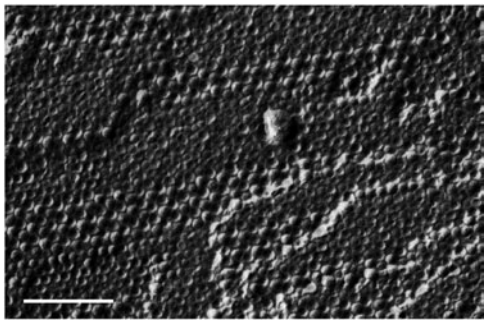

Figure 13. A freeze-fracture electron micrograph of a highly ordered gel phase for a sample of composition 182 mM Na isostearate/567 mM 1-octanol in a H_2O/glycerol mixture that contains 20 wt% glycerol. The bar corresponds to 200 nm.

in temperature. It is located between a lamellar phase and a reverse hexagonal phase. SAXS experiments were in agreement with an fcc cubic structure composed of vesicles with a diameter of 106 Å. However, it is interesting to note that this research was not followed up for a long time and the existence of such highly ordered vesicle gels was not really noticed (it should also be noted that in the original article the constituent particles were not called vesicles, but described as 'structure of spheres in water continuum and consisting of a double layer of amphiphile around a water nucleus' [221]).

More recently we have studied a similar system, i.e. Na oleate/octanol/water, where also SUV are formed for an octanol:Na oleate molecular ratio of about 3:1. If the total concentration is high enough, i.e. above a concentration of 160 mM Na oleate, these vesicles will be densely packed and form a rigid and elastic gel [222], that even exhibits the ringing phenomenon that is frequently encountered for cubic phases of surfactants [223]. At this point it should be noted that these vesicle gels are transparent and isotropic. This is in contrast to vesicle gels that are formed by MLV, that are birefringent and typically exhibit a pronounced stress-induced birefringence [146, 224].

The transparent vesicle gels differ markedly in macroscopic appearance from the vesicle gels of the MLV, as they are much stiffer. This difference can be quantified by rheological measurements and the shear modulus G_0 is in the range of 1000–10 000 Pa and therefore about a factor 100 higher for this new gel phase in the Na oleate system compared to the values observed for the MLV described before. Evidently the elastic properties are much more pronounced in the case of the gels of unilamellar vesicles of the oleate system.

A structural investigation of this vesicle phase shows that here one indeed has a densely packed and highly ordered structure of monodisperse unilamellar vesicles [225]. The high degree of ordering can be seen in figure 13 which is a freeze-fracture electron micrograph of a sample of composition 182 mM Na isostearate/567 mM 1-octanol. The radius of the vesicles is about 17 nm and they are densely packed on a cubic lattice.

SANS experiments show a very peculiar broad double peak with a relatively pronounced minimum in between the peaks (figure 14). This scattering pattern can be explained on the basis of that of densely packed shell-like particles for which the minimum of the form factor of the shells coincides in its q-value with the correlation peak. Accordingly, this superposition of form factor and structure factor leads to a split of the correlation peak into two peaks provided that the monodispersity of the vesicles is large enough to produce a sharp minimum in the particle form factor. This will be the case if the standard deviation of the size distribution is below 10–15%.

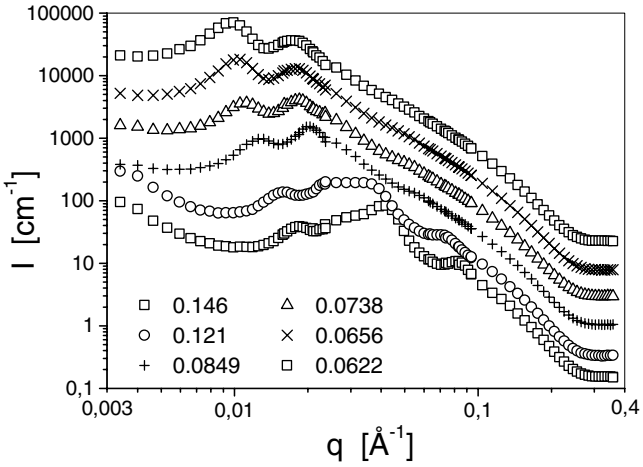

Figure 14. The radially averaged SANS intensity as a function of the scattering vector q for a series of samples with a constant Na oleate/1-octanol molar ratio of 1:3.1. The volume fraction of amphiphilic material (Na oleate + 1-octanol) is given in the inset.

Dilution of such a gel phase with water is possible but only up to a certain total concentration beyond which the gel dissolves and further dilution yields a low-viscosity isotropic liquid. Systematic SANS experiments along such a dilution line show that the size of the vesicles depends on the volume fraction Φ_s of amphiphilic material (figure 14). A very different behaviour is observed for the region of the stiff gel phase and that of the isotropic solution. In the gel phase a shift of the characteristic minimum with decreasing volume fraction towards smaller q-values is observed; i.e. the vesicles are growing in size. Contrary to this, within the isotropic solution no such shift is observed. The minimum remains in place; i.e. the vesicles do not change in size. Only the intensity maximum moves, to lower q-values, which indicates that the interparticle spacing increases upon further dilution, in agreement with a dilution of particles that remain constant in size.

From the position of this intensity minimum, the size of the vesicles can be deduced from the SANS spectra and it is in very good agreement with the radii deduced from electron microscopy. One finds that within the gel phase, a continuous increase in vesicle size upon dilution is observed that follows an experimental scaling law for the radius of $R \sim \Phi_s^{-0.96}$; i.e. the vesicle size is inversely proportional to the amphiphile concentration (figure 15). This value is close to the value -1 that would be expected for vesicles of a given constant bilayer thickness that keep a constant vesicle volume fraction Φ_v, which is defined as the sum of volume fractions of entrapped water plus the amphiphilic bilayer. The scaling law for such a swelling process that keeps the effective packing fraction constant is given by equation (12a) for the case of an infinitely thin shell (where v_s and a_s are the volume of the surfactant and its head group area, respectively) and by equation (12b) for a finite shell thickness D, where Φ_s is the volume fraction of amphiphile:

$$R = (6v_s/a_s)(\Phi_v/\Phi_s) \tag{12a}$$

$$R = 3D(\Phi_v/\Phi_s)\left[0.5 + \sqrt{0.25 - (\Phi_s/3\Phi_v)}\,\right]. \tag{12b}$$

However, the vesicles swell upon dilution with water only until a maximum size is reached, which for the Na oleate is a radius of 23 nm, and for the Na isostearate 15 nm. Further dilution does not lead to a further increase in vesicle size but instead the vesicle gel 'melts' into a dispersion of vesicles, i.e. the observed isotropic solution. Evidently for the vesicles of this

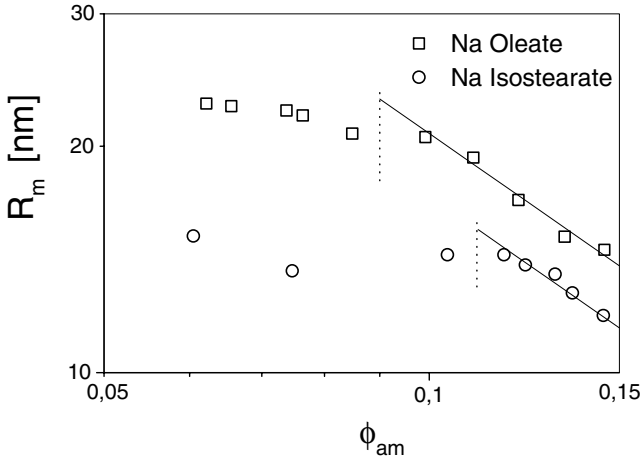

Figure 15. A double-logarithmic plot of the vesicle radius R as a function of the volume fraction Φ of amphiphilic material (Na oleate (isostearate) + 1-octanol) for a constant Na oleate (isostearate)/1-octanol molar ratio of 1:3.1.

system there exists an upper limit for the size beyond which stable unilamellar vesicles are not formed.

This inverse proportionality between vesicle size and amphiphile concentration in the gel phase is also consistent with the rheological data for the gel phase. For the shear modulus G_0 as a function of amphiphile concentration, one observes that it increases with a scaling law according to $G_0 \sim c_s^{2.7}$ (figure 16). Such a scaling law would be expected for a system of densely packed vesicles if one assumes that each vesicle acts as a network point in the gel that stores an elastic energy proportional to kT per vesicle. For such a system the shear modulus G_0 will be given by equation (7): $G_0 = \chi {}^1N kT$, where ${}^1N$ is the number density of the vesicles. If the vesicle radius is inversely proportional to the amphiphile volume fraction Φ_s (as observed by means of SANS), then ${}^1N$ has to be proportional to Φ_s^3, which explains the observed scaling.

Such a scaling of $G_0 \sim R_v^{-3}$ has been similarly observed for densely packed phospholipid unilamellar vesicles with a radius 200–250 nm. In that system, shear moduli of about 10 Pa were observed [82]. The two values are in good quantitative agreement if one considers that the two systems differ in size by about a factor 10, which explains why the moduli differ by a factor 1000. However, it should also be noted that the proportionality factor χ is 30–50 for both systems, which means that each vesicle stores an elastic energy of 30–50 kT. This proportionality factor is expected to be related to the packing of the vesicles and their effective interaction, and similar values have been observed for other vesicle systems [82, 209, 216]. In a first approximation, one may relate the observed shear modulus G_0 to the structure factor at zero-scattering angle $S(0)$, i.e. to the osmotic compressibility $(\mathrm{d}\Pi/\mathrm{d}V)$ of the vesicle system (in this approximation, the shear modulus G_0 has been set identical to the compression modulus K, which corresponds to a value for the Poisson number of 0.125, i.e. a relatively strongly compressible system—as may reasonably be expected for such a vesicle system):

$$G_0 = \frac{{}^1NkT}{S(0)} = \frac{1}{V}\left(\frac{\mathrm{d}\Pi}{\mathrm{d}V}\right)_T. \tag{13}$$

If one assumes that the main interaction in a densely packed vesicle system is due to the steric hindrance, one may describe the interactions by a hard-sphere model for which the

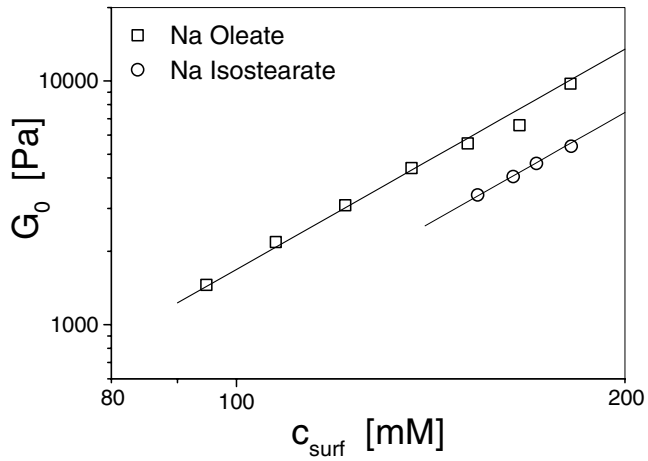

Figure 16. The shear modulus G_0 for samples of constant Na oleate (isostearate)/octanol = 1:3.1 molar ratio as a function of the surfactant concentration.

structure factor for a hard-sphere volume fraction Φ is described by the Carnahan–Starling equation [226]:

$$S(0) = \frac{(1-\Phi)^4}{(1+2\Phi)^2 - 4\Phi^3 + \Phi^4}. \tag{14}$$

The experimentally determined vesicle volume fraction in the gel phase is ∼0.4 and, if one includes a hydration shell with a thickness of 4 Å, the volume fraction becomes 0.44, for which we can calculate an $S(0)$ value of 0.030. This value is in excellent agreement with the experimentally observed proportionality factor of 30–50, which means that the experimentally observed shear modulus can be explained by a simple model of densely packed hard spheres. This is also consistent with the experimental observation that addition of moderate amounts of salt does not influence the value of the shear modulus, which demonstrates that the shear modulus is not controlled by electrostatic interactions but by the packing fraction of the vesicles.

It should be noted here that the formation of the vesicle gel depends in a decisive manner on the surfactant employed. Very similar phase behaviour is observed when Na oleate is substituted for with Na isostearate, but for Na linolate no vesicle gel at all was observed [227]. Despite the fact that all of these surfactants are C_{18} carboxylates, evidently the tendency to form such a vesicle gel depends strongly on the details of the architecture of the amphiphilic molecule. It has also been studied how much of the oleate can be replaced by another surfactant while still retaining the gel phase. Here it has been observed that up to 50 mol% of the oleate can be replaced by TDMAO (tetradecyldimethylamine oxide) or C_{16} DMAO (hexadecyldimethylamine oxide) without destroying the vesicle gel phase and without reducing its elastic properties [227].

SANS measurements on such samples for various degree of substitution show that the basic structure of the vesicle gel is retained, as can be seen from the similarity of the scattering curves. Only for the highest degree of 50 mol% substitution does one observe that the scattering pattern changes significantly, and here the bump between the two scattering peaks has vanished. This indicates that for this sample the polydispersity of the vesicles has increased significantly and this pronounced increase of polydispersity explains why for higher degrees of substitution a highly ordered vesicle gel can no longer be formed, as such more polydisperse vesicles will only be able to form a more glass-like structure.

The vesicle gel is much more sensitive to an increase of the ionic strength. Addition of up to 5–10 mM NaCl does not influence the shear modulus G_0, but higher salt concentrations lead to a pronounced decrease of the elastic properties; i.e. the gel becomes transformed into a sol state. Evidently the influence of the increasing ionic strength on the shear modulus is less due to a reduced interaction between the aggregates, as then there should be a continuous decrease, than to the vesicles themselves. As long as they remain intact, the shear modulus remains constant, and therefore is given by their number density and packing which are unaffected for low salt content. As soon as a certain threshold of the ionic strength is surpassed, the monodispersity of the vesicles is altered drastically as can be inferred from SANS measurements. Now these much more polydisperse vesicles are no longer able to sustain the dense packing, and therefore the shear modulus is reduced drastically.

Another interesting observation concerns the possibility of the replacement of the cosurfactant 1-octanol by an alcohol of different chain length. This is possible without any problem for the case of 1-hexanol or 1-heptanol where, for samples with equal volume fractions of alcohol, basically identical vesicle gels are formed which possess the same rheological properties. However, for 1-pentanol a viscous isotropic phase is obtained and for 1-nonanol and 1-decanol turbid viscous phases are obtained that show streaming birefringence and contain MLV. Evidently the ratio of the chain lengths of the surfactant and cosurfactant has to be in a certain range. For longer or shorter cosurfactant chains the conditions for the formation of SUV are not given and correspondingly no densely packed vesicle gel can be formed.

The formation of gels of SUV can also be induced by the addition of an oppositely charged polyelectrolyte to catanionic vesicles. This has been demonstrated for the addition of cationic polyelectrolytes derived from hydroxyethylcellulose [228].

Finally, it might be added that the formation of organogels with a solvent DMSO/water mixture has also been reported, which consist of networks of polymer-coated vesicles where the vesicles are composed of a cholesterol–saccharide compound [229]. These vesicles are held together by a boronic acid-appended poly(*L*-lysine), where in this system the polymer effectively functions as a cross-linker for the vesicles.

4. Dynamics of formation

So far we have been concerned with situations in which surfactant systems form vesicles or, for more concentrated systems, vesicle gels. Another interesting approach is not only to consider the conditions for which vesicles are formed spontaneously but also to study the pathways via which they are formed. In general, transitions between different amphiphilic structures have not been studied intensively and there exist only a small number of time-resolved investigations of the dynamic processes that occur during such structural transformations. Accordingly, only little is known about the structural pathways via which morphological transitions take place and what the physico-chemical parameters that control them are.

4.1. An overview of dynamic experiments performed

In many situations, vesicles can be formed spontaneously by changing parameters such as composition or temperature. A change of composition can very easily be brought about by mixing corresponding starting systems. In many such circumstances, bilayer and vesicle formation can be brought about from starting solutions that contain no bilayer structures themselves but, for instance, are micellar solutions. Therefore it is already interesting in itself to study how these morphological changes of amphiphilic systems take place, i.e. via which structural intermediates these morphological transitions proceed. Moreover, the understanding

of the kinetic pathways and the intermediate structures involved is also important, as in many circumstances the vesicles formed may only be metastable structures and therefore their structure will depend strongly on their formation process. A detailed understanding of the formation process will accordingly allow one to control the vesicle structures formed.

The structural changes may be followed by methods that allow indirect detection, such as electric conductivity and turbidity methods, or be they can be monitored by methods of structure observation, such as direct visualization (light or electron microscopy) and scattering techniques (light, x-ray, or neutron). However, simple mixing and subsequent observation is only a feasible approach for systems that react relatively slowly, e.g. amphiphilic block copolymers [230]. Typically, low-molecular-weight amphiphiles exhibit much faster kinetics and for such systems the different components have to be mixed quickly in order to observe a structural change. Here the stopped-flow technique [231] is a method of choice, as it allows rapid mixing with dead times of around 1–10 ms.

In some circumstances the transition from micelles to vesicles can be slow enough to be followed by cryo-transmission electron microscopy (TEM). This is the case for the solubilization of lecithin vesicles by a cationic surfactant, cetyltrimethylammonium chloride (CTAC), where time-resolved cryo-TEM experiments were able to demonstrate a vesicle growth that takes place during several hours after the addition of CTAC to lecithin vesicles that were prepared by sonication. It could also be shown that this growth process takes place via an intermediate state comprising open bilayer discs [232]. Similar investigations were also carried out with alkylsulfates as the solubilizing surfactant [233]. Here it was observed that the chain length of the surfactant strongly influences not only the amount of surfactant needed for the solubilization of the lipid bilayer but also the type of the intermediate structures formed during the vesicle-to-micelle transition. For decylsulfate a coexistence of a normal lamellar (L_α) phase with rod-like micelles was observed, whereas for dodecylsulfate and tetradecylsulfate a holey lamellar phase was observed.

The process of vesicle formation from mixtures of cationic and anionic surfactants is in some cases slow enough to be followed easily. For instance, vesicle formation has been studied by means of time-resolved turbidity, dynamic light scattering, and cryo-TEM experiments when CTAB is mixed with sodium octyl sulfate (SOS) or dodecyl benzene sulfonic acid (HDBS). For the system CTAB/SOS, formation of equilibrium vesicles takes several hours to months, while for CTAB/HDBS, the process is complete within several minutes. These experiments showed that the intermediate-state aggregates are worm-like micelles and discs, i.e. the micelles grow to form floppy, undulating discs [234]. Once these discs reach a critical disc size, a transition to SUV takes place that is driven by competition between the edge energy of the discs and the bending energy required to form spherical structures [235]. Such a critical disc size prior to vesicle formation could also be inferred from cryo-TEM experiments on mixtures of CTAB and sodium perfluoro-octanoate where bilayer discs are in equilibrium with SUV and bilayer cylinders [236]. Also for this case it could be shown that the critical disc size is related to the bending moduli of the corresponding amphiphilic bilayer and it is interesting to note that the discs contain much less material than is required for the formation of the SUV that they are in equilibrium with.

Another case that has been studied in much detail is the vesicle formation in aqueous micellar mixtures of lecithin and bile salt that takes place upon dilution with water. On dilution, the relative amount of the more soluble bile salt in the mixed aggregates will be reduced. Correspondingly, the preferred curvature of the aggregates is reduced, until at a critical composition a transition to bilayers takes place—i.e. unilamellar vesicles are formed spontaneously [237, 238]. This transition has been studied intensively by means of time-resolved scattering methods (static and dynamic light scattering, SANS) and it has been

concluded that this transition takes place via elongated micelles and disc-like micelles as intermediate structures [239–241]. More recent experiments by means of time-resolved static and dynamic light scattering on such aqueous lecithin/bile salt mixtures show a strong dependence of the kinetic rates and the final state of the vesicles formed on the total amphiphile concentration and on the ionic strength. The experimental observations disagree with equilibrium calculations. However, this can be explained quantitatively by means of a kinetic model, where the key steps are a rapid formation of disc-like intermediates, growth of these discs, and their closure to form SUV; i.e. the transition is controlled kinetically rather than thermodynamically and this applies also to the final state that is assumed by the amphiphilic system [242]. It should be added here that a recent investigation on the lamellar-to-vesicle transition that occurs in a phospholipid system upon dilution showed that the size of the unilamellar vesicles formed is related to the wavelength of in-plane undulations of the lamellar phase that borders on the vesicle phase to slightly higher concentrations [243].

The micelle-to-vesicle transition in mixtures of phospholipids and bile salt can not only be achieved by dilution but also by a temperature jump. Small-angle x-ray scattering (SAXS) has been used to study the process of formation of unilamellar vesicles that was induced from the micellar solution by temperature jumps with heating rates of 5–100 K min^{-1} [244]. The transition has been shown to be reversible. The rate of temperature change is crucial for the type of vesicles that are formed. Slow temperature changes yield large and polydisperse vesicles while fast temperature variations lead to small and monodisperse vesicles that increase in size upon cooling.

However, in many situations the transitions of interest take place on a much faster timescale and cannot be studied by means of simple mixing and consecutive structural investigations. In order to study the kinetics of such fast transitions, rapid mixing techniques such as the stopped-flow method have to be employed. For instance, this has been done for a similar system of lecithin and sodium xylenesulfonate that forms micellar solutions at higher concentrations and is transformed into vesicles by dilution. The structural changes were detected by means of light scattering and electric conductivity measurements and showed that the vesicle formation takes place by the agglomeration of fragments [245].

Stopped-flow experiments have been used to study the vesicle breakdown that takes place upon dilution of solutions of vesicle-forming sodium tridecyl-6-benzene sulfonate (STBS). The kinetics was followed by means of turbidity measurements, and typical breakdown times for the vesicles were found to be 0.1–10 s with an activation energy of $\sim$60 kJ mol^{-1}. For this case also disc-like aggregates are proposed as intermediate structures [246]. The STBS vesicles can also be destroyed by titration with single-chain surfactants such as SDS. Here the transition occurs more slowly and could be followed by turbidity measurements after conventional mixing [247]. The rate of vesicle formation/breakdown depends on how far the final concentrations are from the phase transition concentration required for the process of formation/breakdown of the vesicles, i.e. the driving force that determines the kinetics of the process is proportional to the distance of the final composition from the composition required to achieve the structural transition [248]. By performing similar experiments on the vesicle breakdown of catanionic and double-chain cationic vesicles induced by the addition of single-chain surfactants, this driving-force concept could be corroborated and generalized [249].

The vesicle formation that takes place after mixing cationic and anionic surfactant solutions has been investigated by means of stopped-flow experiments coupled to time-resolved light scattering experiments. These experiments, that were done on mixtures of CTAB/SOS and dodecyltrimethylammonium bromide (DTAB)/SDS, showed that the process of vesicle formation consists of a series of first-order events, the slowest being the relaxation of the non-equilibrium vesicles formed initially to their final size and size distribution [250].

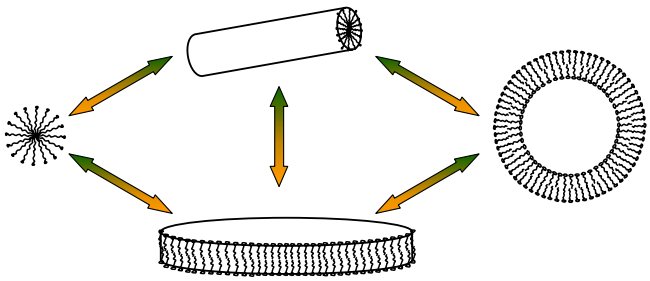

Figure 17. A schematic representation of the pathways that may be involved in the transition from micelles to unilamellar vesicles.

This various pieces of experimental evidence for the structural changes during the micelle ↔ vesicle transition can be summarized schematically as in figure 17 with rod-like and/or disc-like aggregates as intermediate structures. However, it should be noted that only little is known about the detailed structure of the intermediate aggregates and the details of the structural transformations will certainly depend subtly on the composition of the amphiphilic systems involved and the way in which the transition is induced.

Having reviewed some of the published investigations on the kinetics of vesicle formation/breakdown, we now want to discuss in the following some results that were obtained by us by coupling the stopped-flow technique with highly time-resolved scattering methods: SAXS and SANS experiments. By means of SAXS experiments we have studied the process of mixing of a cationic and an anionic surfactant solution. By means of SANS we followed the vesicle formation that takes place in an anionic surfactant solution after addition of a cosurfactant.

4.2. An example of catanionic vesicles

For our investigation of the formation of catanionic vesicles, we chose as our example mixtures of tetradecyltrimethylammonium hydroxide (TTAOH) as the cationic surfactant and dodecylethoxysulfonic acid (Texapon N_{70}-H, Tex-H, $C_{12}H_{25}$–$(OC_2H_4)_{2.5}$–O–SO_3H) as the anionic surfactant. A very interesting feature of this mixture is the fact that a salt-free catanionic system is formed because the counterions of the surfactants recombine to form water. This renders it a particularly simple system with well-defined electrostatic conditions.

Time-resolved SAXS experiments were performed on the ID-2 instrument of the ESRF, Grenoble, France [251]. The high flux and a 2D CCD detector allowed us to obtain SAXS spectra of good quality with acquisition times down to 20 ms while the dead time of the stopped-flow device was about 5 ms.

As a representative system, the mixing of 100 mM solutions of TTAOH and Tex-H at the equimolar ratio was studied. The starting solutions are of low viscosity and contain small micelles. SAXS experiments on the pure starting solutions (figure 18) show for the 100 mM Tex-H solution a minor maximum at $q \approx 0.47$ nm^{-1} and a main maximum at $q \approx 1.44$ nm^{-1}, while for the 100 mM TTAOH solution only one peak is observed, at $q \approx 0.83$ nm^{-1}. For TTAOH, with its relatively homogeneous electron density, this is the correlation peak of the charged micelles, as is the first, less pronounced peak for the Tex-H (the main peak is due to the maximum of the form factor since for the Tex-H the electron density distribution is dominated by the sulfate head group) [252]. From the q-position, one can deduce the mean radius of the TTAOH micelles to be 16.2 and 27.1 Å for the Tex-H, i.e. for both surfactants small micelles are present. However, in the phase diagram of TTAOH/Tex-H/H_2O for a total surfactant concen-

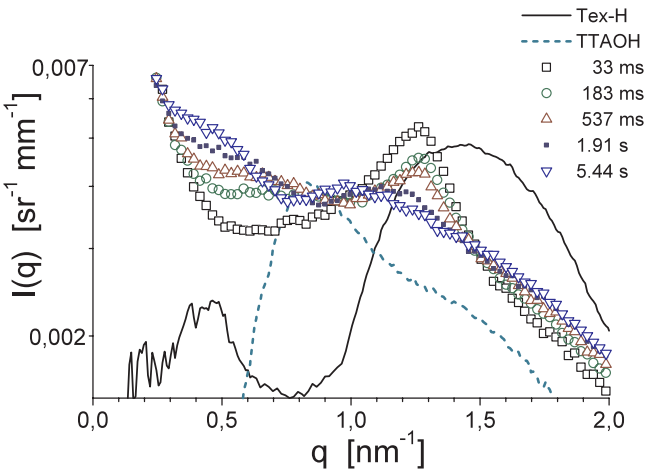

Figure 18. SAXS intensity curves for 50 mM Tex-TTA for various times after mixing in the stopped-flow cell. In addition, the scattering curves for the pure 100 mM TTAOH and Tex-H solutions are given.

tration of 100 mM, a vesicle phase is observed for equimolar mixtures, which extends to more than a molar ratio of 3:2 in favour of either one of the two components. Dynamic light scattering experiments showed that these vesicles have a hydrodynamic radius of 125–130 nm [253]. Evidently, upon mixing, the small micelles are transformed into large vesicular aggregates.

The transition of the micelles to unilamellar vesicles was followed by means of time-resolved SAXS experiments. In figure 18 scattering curves of the time-resolved SAXS experiments for the large-q range are given for various times after mixing equimolar amounts. Immediately after the mixing, a transient intensity maximum appears at $q \approx 1.25$ nm^{-1} that vanishes with a time constant of 580 ms. This correlation peak is due to micellar aggregates that are present shortly after the mixing. The peak is located between those of the pure surfactant solutions, somewhat closer to that of the pure 100 mM Tex-H. Evidently the mixed micelles have a size intermediate between those of the pure starting solutions and are formed on a timescale shorter than can be resolved by this experiment, i.e. faster than 10 ms. After this transient peak has disappeared, the scattered intensity becomes a continuously decreasing function of q with a scattering behaviour that is typical for surfactant bilayers. A bilayer thickness of 4.1 nm could be deduced from the scattering experiments, which is in good agreement with twice the length of the stretched surfactant molecules. It should be noted that by means of such time-resolved SAXS experiments, one is able to follow directly the micellar dissolution process [253].

From these experiments it could also be deduced that apparently, in the beginning, mixed micelles are formed that are not equilibrated with respect to their ionic charges. However, the charge equilibration takes place on a faster timescale than the disintegration of the complete micelles. This is reasonable, since for the charge equilibration it is sufficient that oppositely charged surfactant monomers diffuse into the micelle which is fast process and additionally driven by electrostatic attraction. For the complete disintegration of the micellar aggregates, it is necessary not only that monomer exchange takes place but also that at intermediate stages very small micelles are formed. However, the probability for such small micelles forming is very low and accordingly the process of micellar disintegration occurs more slowly, which is in agreement with classical micellar kinetics [254, 255].

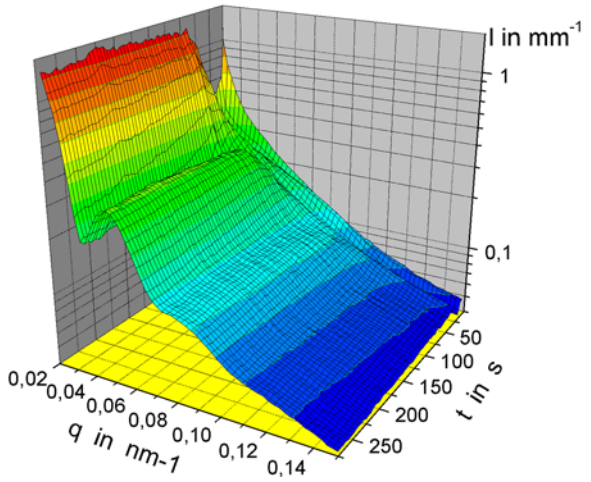

Figure 19. The temporal evolution of the SAXS intensity in the small-q range for a system of 50 mM Tex-TTA at 25 °C after mixing.

However, even more interesting than the micellar disintegration process is the formation of the unilamellar vesicles that should be present at the end. This is observed in the lower-q range and figure 19 displays the temporal evolution of the scattering curves. Already, after a very short time of 100 ms, some scattering from flat objects is observed. It is interesting to note that after about 5 s a minimum in the scattering curves appears around $q = 0.04\ \mathrm{nm}^{-1}$. Subsequently this minimum moves to somewhat lower q and becomes more pronounced with time, i.e. second- and third-order intensity oscillations become visible. The oscillating scattering patterns in figure 19 are characteristic for shell-like particles and can be fitted well with the form factor of polydisperse shells of thickness d with a Schulz size distribution $f(r)$. The resulting expression for the scattering intensity can be written as

$$I(q) = {}^1N \int_0^\infty \mathrm{d}r\ f(r) P(q, r) \tag{15}$$

where ${}^1N$ is the number density of vesicles, and $f(r)$ and $P(q, r)$ are given by

$$f(r) = \left(\frac{t+1}{R_m}\right)^{t+1} \frac{r^t}{\Gamma(t+1)} \exp\left(-\frac{t+1}{R_m} r\right) \tag{16}$$

with R_m the mean radius, and the polydispersity is characterized by $t + 1 = 1/p^2$, where p is the polydispersity index ($p^2 = (\langle \Delta R^2 \rangle / R_m^2) - 1$), and

$$P(q, r) = 16\pi^2(\rho_A - \rho_S)^2\{(r + d/2)^3 f_0(q(r + d/2)) - (r - d/2)^3 f_0(q(r - d/2))\}^2 \tag{17}$$

with

$$f_0(x) = (\sin x - x \cos x)/x^3.$$

ρ_A and ρ_s are the scattering length densities for bilayer and solvent, respectively. The bilayer thickness d was determined as 4.1 nm. From fitting this model to the experimental data, the mean radius R_m and the polydispersity index p were obtained. Their evolutions as a function of time are given in figure 20. One observes that R_m increases from about 75 to 85 nm, while at the same time p decreases from more than 0.2 down to 0.15. The final mean radius R_m of 85.6 nm with a polydispersity index of 0.157 corresponds perfectly well to the hydrodynamic radius R_h (z-average) obtained by dynamic light scattering for conventionally

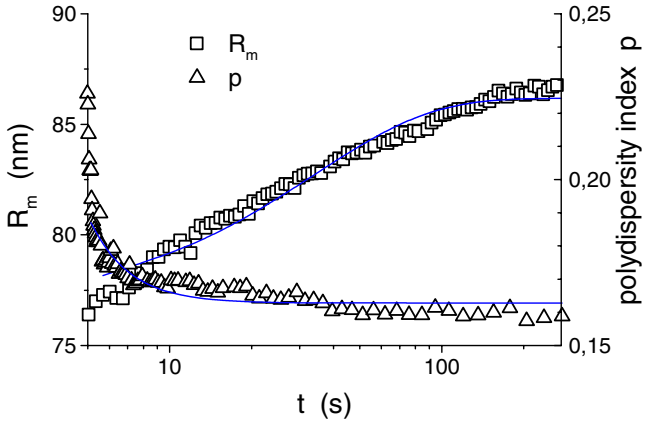

Figure 20. The mean radius R_m and polydispersity index p for 50 mM Tex-TTA as a function of time. Solid curves are single exponentials with $\tau = 22.4$ s (p) and $\tau = 28.5$ s (R_m).

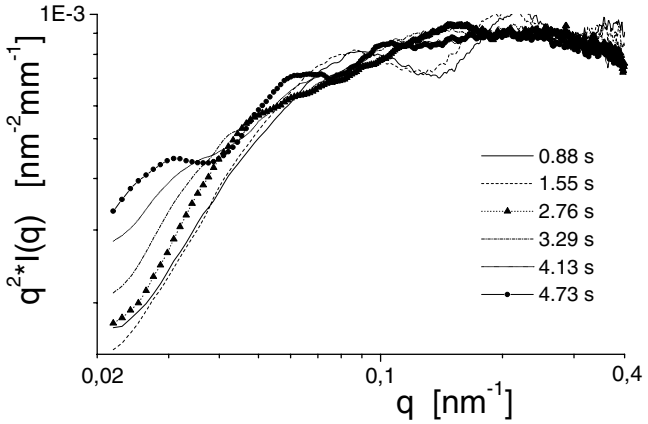

Figure 21. A Kratky–Porod plot for 50 mM Tex-TTA for the intermediate time range of 1–5 s after mixing.

prepared samples; i.e. in the stopped-flow experiment the same final size was achieved as for simple mixing and homogenization of the sample. The temporal change for both quantities can be described by a single-exponential function and the time constants for the change of radius and polydispersity are similar, i.e. about 25 s. From this it can be concluded that the process of formation of the unilamellar vesicles takes place on a much slower timescale than the dissolution of the mixed micelles originally present.

From the results presented so far, it is clear that the micelles initially present disappear within less than a second but the first vesicles are only discerned after more than 5 s. Obviously, in between there must be an intermediate state. A Kratky–Porod plot of the scattering curves at intermediate times (figure 21) demonstrates that even after short times of much less than a second a locally flat structure is observed, as evidenced by the plateau value at higher q (in this representation, a constant value would be expected for an infinitely extended flat structure).

However, lower intensity values are observed for the lower-q range that increase with time. Another interesting feature of the scattering curves is the oscillations in the q-range of 0.08–0.4 nm^{-1} that change systematically with time. All this indicates that there exists a well-defined intermediate structure prior to the formation of vesicles.

Such scattering curves are typical for the scattering of disc-like objects and can be fitted with a disc model according to

$$I(q,t) = A(t)P_{disc}(q, R_d, D) + B(t)P_{sp}(q, R_{sp})S_{chsp}(q, R_{sp}) \tag{18}$$

where A and B are time-dependent amplitudes for the form factors of discs and initially present spherical micelles that indicate the relative amount of amphiphilic material that is present in the different morphologies. The most interesting quantity obtained from these fits is the disc radius R_d that increases linearly with time from 20 to 35 nm for times between 1 and 5 s until the formation of vesicles is observed in the scattering curves [256]. This clearly demonstrates that disc-like micellar aggregates are formed as an intermediate structure well before the formation of vesicles starts. A very interesting feature is the fact that the discs only grow up to a maximum value for R_d of 35–40 nm, which is less than half the radius of the vesicles that are formed at the same point of time. Obviously, one reaches here a critical upper value for the disc size beyond which the formation of closed bilayer vesicles is energetically favoured. This is in agreement with an observation that has been made for mixtures of cetyltrimethylammonium bromide (CTAB) and sodium perfluoro-octanoate, where an equilibrium between disc-like micelles and unilamellar vesicles has been observed where the discs also contain much less amphiphilic material than the vesicles.

4.3. An example of ionic surfactant/cosurfactant vesicles

However, the formation of disc-like intermediates is not necessarily a required prerequisite for the formation of vesicles, as had already be seen from the literature survey. For that purpose, we studied another system that also forms vesicles but is composed of an ionic surfactant (sodium oleate) and a cosurfactant (1-octanol). This system forms an extended vesicle phase in the concentration range of 80–250 mM sodium oleate [224]. In order to study the process of formation of the vesicles, time-resolved SANS experiments with a time resolution of 100 ms were carried out with a stopped-flow device on the D22 instrument of the ILL, Grenoble, France [257]. Vesicle formation was induced by mixing a surfactant solution directly with a corresponding amount of 1-octanol. Initially, small emulsion droplets of octanol are formed that become dissolved in the surfactant solution in the course of time, thereby forming vesicles.

Scattering curves for various times after the mixing process for a 100 mM Na oleate solution with 3.5 wt% 1-octanol are shown in figure 22. The emulsion droplets are responsible for an increase of scattering intensity at low q-values. For the micellar correlation peak, one observes that with passing time it shifts continuously to lower q-values. The change of the scattering curves can be associated with the growth of rod-like micelles. The length of the rods can be deduced from a quantitative analysis, and it follows roughly a linear growth law for short times [256]. The scattering from vesicles can only be discerned after about 2 min. It is seen as a dent in the scattering intensity in the range 0.02–0.025 $Å^{-1}$ and one can deduce that the vesicles formed have a radius of about 150 Å [258]. It is interesting to note that the rod-like micelles only grow to about a length of twice the vesicle radius before closure and formation of vesicles is observed. Evidently in this case of vesicle formation, no disc-like intermediate is assumed, but instead one observes a direct transition from rod-like micelles (that presumably become biaxial during their growth process) to SUV. A quantitative analysis of the scattering curves shows that the vesicles formed grow somewhat in size and become more monodisperse with time. However, after about 1 h, no further changes are observed and the SUV finally

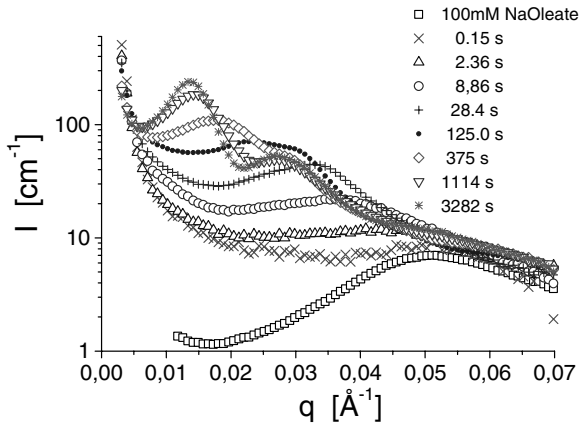

Figure 22. The SANS intensity for 100 mM Na oleate after addition of 3.5 wt% 1-octanol. For comparison, the pure 100 mM Na oleate is also included.

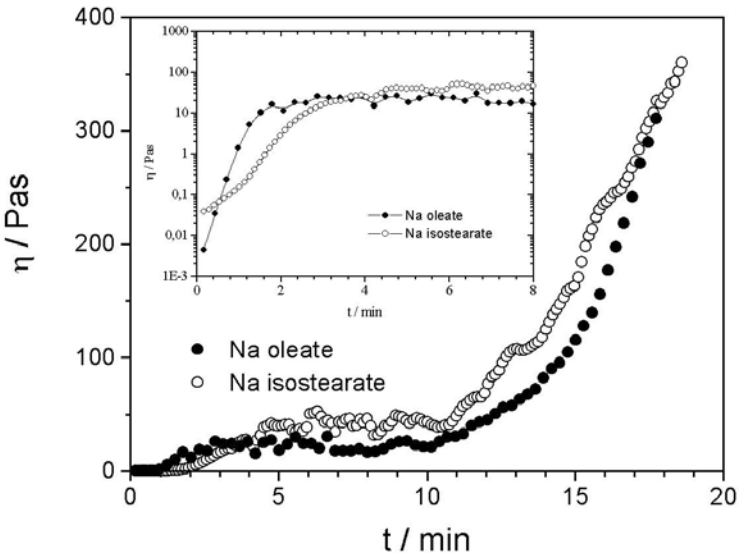

Figure 23. The viscosity η (at a shear rate of 0.22 s^{-1}) as a function of time for the gelation process of a sample of composition 182 mM Na oleate (●) (isostearate: ○)/567 mM 1-octanol at 25 °C.

formed have a mean radius of 140 Å, a bilayer thickness of 22 Å, and a polydispersity index of 0.15.

For the same system (Na oleate or Na isostearate plus 1-octanol), for larger concentrations the formation of a highly ordered vesicle gel has been observed [224]. This vesicle gel can be conveniently prepared by simple vortexing of the corresponding surfactant solution with a given amount of added 1-octanol. The formation of the gel phase was studied by means of viscosity and other rheological measurements and also by means of SANS experiments [259]. Time-resolved viscosity measurements on identically composed systems (187 mM surfactant/567 mM 1-octanol) with either Na oleate or Na isostearate exhibit very similar behaviour (figure 23). For short times a rapid increase by about three orders of

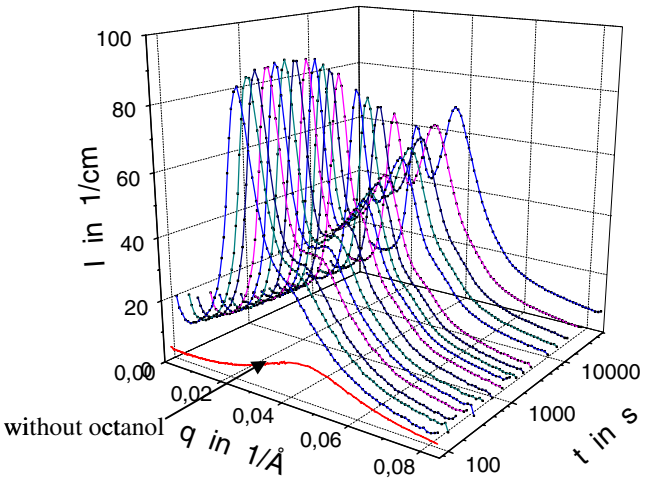

Figure 24. SANS curves for a sample of 182 mM Na isostearate/567 mM 1-octanol in D_2O at 25 °C taken at various times after mixing the sample. In addition, the scattering curve for the sample prior to octanol addition is given.

magnitude takes place that is faster for the oleate (∼60 s) than for the isostearate (∼150 s). Afterwards a plateau of constant viscosity of 15–30 Pa s is reached and only more than 10 min after the mixing is a further increase of viscosity observed. For both systems the viscosity diverges after ∼18 min; i.e. here the systems have gelled.

SANS curves for a sample with a final composition of 182 mM Na isostearate/567 mM 1-octanol in D_2O show a drastic change of within the first 2.5 min, after which a much higher scattering intensity and a completely different shape of the curve are observed (figure 24). From the experiments on the more dilute systems, it is clear that during this time the formation of vesicles has taken place. After a few minutes, one can already discern the scattering pattern of relatively monodisperse vesicles that are characterized by a minimum in the region of high intensity, i.e. for $q \sim 0.03$ Å^{-1}. However, unlike in the more dilute case, the scattering pattern is still changing after several hours and even over several days. The interpretation of this behaviour is that the SUV initially formed produce a vesicle gel within less than 20 min. This vesicle gel has a glass-like ordering, but after the gelation the SUV still grow somewhat in size and become more monodisperse (as can be seen from the intensity minimum that becomes more pronounced and moves to lower q-values). These more monodisperse SUV are now able to pack in a more highly ordered fashion, as can be seen in the final structure (cf figure 13). However, this structural rearrangement can only occur on a relatively slow timescale, since the system is already in a glassy state and the structural rearrangement is now strongly hindered by the high local viscosity experienced by the vesicles.

It might be added here that vesicle gels of densely packed SUV have also been reported for phospholipids. They can be obtained by high-pressure homogenization of highly concentrated phospholipid dispersions [260]. Dilution of these gels with water leads either to MLV or SUV depending on the dilution technique applied [261].

5. Summary and outlook

In conclusion, it can be stated that vesicles and vesicle gels are highly interesting cases of self-organizing structures that are of key importance for a large variety of different

applications. They can be formed by substantially different amphiphiles and may range in size from ultrasmall unilamellar vesicles (USUV) with radii of 4–10 nm up to large unilamellar vesicles (LUV) and multilamellar vesicles (MLV) of more than 20 μm diameter. Their rich morphological diversity renders them extremely versatile colloidal structures that may exhibit broadly different properties.

Although, classically, vesicles are formed by application of external forces, there now exists abundant evidence for spontaneous vesicle formation and there are also many indications that, at least in some situations, the vesicles formed (this applies mainly to unilamellar vesicles) may be thermodynamically stable structures.

If they are sufficiently well defined in size, it is possible that they form ordered vesicle gels with a dense packing of spherical objects. Such gels possess pronounced elastic properties even for relatively moderate volume fractions of amphiphile, that can be related to the osmotic compressibility of the system and the bending modulus of the bilayer. We have investigated a case where such a highly ordered elastic vesicle gel is formed by purely diffusive processes after simple mixing of a surfactant solution and a cosurfactant.

The dynamics of the formation of vesicles and vesicle gels is a fascinating topic that can be studied in much detail by time-resolved scattering techniques. The formation of the vesicle gel from surfactant solution and added cosurfactant is a multiple step that involves first a growth of rod-like micelles, then their transformation to vesicles that gel by forming a glassy structure. Only by a much slower ordering process is a highly ordered vesicle gel formed, after more than a day.

In contrast to that process, we observe a pathway where, as intermediate structures, disc-like objects are formed after the mixing of cationic and anionic surfactant solutions that form spontaneously unilamellar monodisperse vesicles. Highly time-resolved SAXS experiments allowed us to follow the dissolution of the micelles that were initially present, the formation of intermediate discs, and the final formation and ripening of the vesicles in a single experiment.

It is to be expected that questions regarding the thermodynamic stability of vesicles will remain a focus of future investigations. Moreover, investigations of the mechanisms of vesicle formation/breakdown will be of great interest, as often in such systems only metastable structures are formed. Therefore control of the vesicle structures and properties is possible by means of controlling their preparation process—provided that the dynamics of the formation process is sufficiently well understood.

Acknowledgment

A referee is thanked for some helpful comments that led to this article being more complete.

References

[1] Ekwall P, Mandell L and Fontell K 1969 *Mol. Cryst. Liq. Cryst.* **8** 157
[2] Wennerström H and Lindman B 1979 *Phys. Rep.* **52** 1
[3] Tiddy G J T 1980 *Phys. Rep.* **57** 1
[4] Chevalier Y and Zemb T 1990 *Rep. Prog. Phys.* **53** 279
[5] Laughlin R G 1994 *The Aqueous Phase Behavior of Surfactants* (London: Academic)
[6] Tanford C 1980 *The Hydrophobic Effect: Formation of Micelles and Biological Membranes* 2nd edn (New York: Wiley)
[7] Israelachvili J N, Mitchell D J and Ninham B W 1976 *J. Chem. Soc. Faraday Trans.* II **72** 1525
[8] Seifert U 1997 *Adv. Phys.* **46** 13
[9] Zilker A, Ziegler M and Sackmann E 1992 *Phys. Rev.* A **46** 7998
[10] Michaelet X and Bensimon D 1995 *Science* **269** 666

[11] Papahadjopoulos D 1978 *Ann. New York Acad. Sci.* **308** 371
[12] Bangham A D and Horne R W 1964 *J. Mol. Biol.* **8** 660
[13] Bangham A D, Standish M M and Watkins J C 1965 *J. Mol. Biol.* **13** 239
[14] Panizza P, Roux D, Vuillaume V, Lu C Y D and Cates M E 1996 *Langmuir* **12** 248
[15] Regev O and Guillemet 1999 *Langmuir* **15** 4357
[16] Israelachvili J N, Mitchell D J and Ninham B W 1977 *Biochim. Biophys. Acta* **470** 185
[17] Schomäcker R and Strey R 1994 *J. Phys. Chem.* **98** 3908
[18] Ekwall P, Mandell L and Fontell K 1969 *Mol. Cryst. Liq. Cryst.* **8** 157
[19] Roux D, Cates M E, Olsson U, Ball R C, Nallet F and Bellocq A M 1990 *Europhys. Lett.* **11** 229
[20] Benton W J and Miller C A 1983 *J. Chem. Phys.* **87** 4981
[21] Lang J and Morgan R D 1980 *J. Phys. Chem.* **73** 5849
[22] Gazeau D, Bellocq A M, Roux D and Zemb T 1989 *Europhys. Lett.* **9** 447
[23] Strey R, Jahn W, Porte G and Bassereau P 1990 *Langmuir* **6** 1635
[24] Porte G, Marignan J, Bassereau P and May R 1988 *J. Physique* **49** 511
[25] Miller C A, Gradzielski M, Hoffmann H, Krämer U and Thunig C 1991 *Prog. Colloid Polym. Sci.* **84** 243
[26] Roux D, Coulon C and Cates M E 1992 *J. Phys. Chem.* **96** 4174
[27] Mitchell D J and Ninham B W 1981 *J. Chem. Soc. Faraday Trans.* II **77** 601
[28] Helfrich W 1973 *Z. Naturf.* c **28** 693
[29] Helfrich W 1994 *J. Phys.: Condens. Matter* **6** A79
[30] Bangham A D 1972 *Annu. Rev. Biochem.* **41** 753
[31] Lipowsky R and Sackmann E (ed) 1995 *Structure and Dynamics of Membranes* (Amsterdam: Elsevier)
[32] McCalden T A 1990 *Adv. Drug. Deliv. Rev.* **5** 253
[33] Lasic D D and Rosoff M (ed) 1996 *Vesicles (Surface Science Series vol 62)* (New York: Dekker) p 447
[34] Felgner P L 1990 *Adv. Drug. Deliv. Rev.* **5** 163
[35] Lasic D D 1997 Liposomes *Gene Delivery* (Boca Raton, FL: Chemical Rubber Company Press)
[36] Szoka F and Papahadjopoulos D 1980 *Annu. Rev. Biophys. Bioeng.* **9** 467
[37] Tadros T F 1993 *Adv. Colloid Interface Sci.* **46** 1
[38] Pavelic Z, Skalko-Basnet N and Schubert R 2001 *Int. J. Pharm.* **219** 139
[39] Papahadjopoulos D and Watkins J C 1967 *Biochim. Biophys. Acta* **135** 639
[40] Johnson S M, Bangham A D, Hill M W and Korn E D 1971 *Biochim. Biophys. Acta* **233** 820
[41] Huang C H 1969 *Biochemistry* **8** 344
[42] Olson F, Hunt C A, Szoka F C, Vail W J and Papahadjopoulos D 1979 *Biochim. Biophys. Acta* **557** 9
[43] Mayer L D, Hope M J and Culles P R 1986 *Biochim. Biophys. Acta* **858** 161
[44] Zasadzinski J A N 1986 *Biophys. J.* **49** 1119
[45] Zhang L and Eisenberg A 1995 *Science* **268** 1728
[46] Zhang L, Bartels C, Yu Y, Shen H and Eisenberg A 1997 *Phys. Rev. Lett.* **79** 5034
[47] Shen H and Eisenberg A 1999 *J. Phys. Chem.* B **103** 9473
[48] Luo L and Eisenberg A 2001 *J. Am. Chem. Soc.* **123** 1012
[49] Jenekhe S A and Chen X L 1998 *Science* **279** 1903
[50] Yu K and Eisenberg A 1996 *Macromolecules* **29** 6359
[51] Luo L and Eisenberg A 2001 *Langmuir* **17** 6804
[52] Zhang L and Eisenberg A 1998 *Polym. Adv. Technol.* **9** 677
[53] Zhang L and Eisenberg A 1999 *Macromolecules* **32** 2239
[54] Wang W, Tetley L and Uchegbu I F 2001 *J. Colloid Interface Sci.* **237** 200
[55] Regen S L, Czech B and Singh A 1980 *J. Am. Chem. Soc.* **102** 6638
[56] Akimoto A, Norn K, Gros L, Ringsdorf H and Schupp H 1981 *Angew. Chem. Int. Edn Engl.* **20** 90
[57] Tundo P, Kippenberger D J, Klahn P L, Pietro N E, Tao T C and Fendler J H 1982 *J. Am. Chem. Soc.* **104** 456
[58] Johnston D S, Sanghera S, Pons M and Chapman D 1980 *Biochim. Biophys. Acta* **602** 57
[59] Ringsdorf H, Schlarb B and Venzmer J 1988 *Angew. Chem.* **100** 117
[60] Neumann R and Ringsdorf H 1986 *J. Am. Chem. Soc.* **108** 4487
[61] Bailey W J and Zhou L L 1992 *Macromolecules* **25** 3
[62] Nardin C, Hirt T, Leukel J and Meier W 2000 *Langmuir* **16** 1035
[63] Meier W, Nardin C and Winterhalter M 2000 *Angew. Chem.* **112** 4747
[64] McKelvey C A, Kaler E W, Coldren B, Jung H T and Zasadzinski J A 2000 *Langmuir* **16** 8285
[65] McKelvey C A and Kaler E W 2002 *Langmuir* **245** 68
[66] Zhou S, Burger C, Chu B, Sawamura M, Nagahama N, Toganoh M, Hackler U E, Isobe H and Nakamura E 2001 *Science* **291** 1945
[67] Donath E, Sukhorukov G B, Caruso F, Davis S A and Möhwald H 1998 *Angew. Chem. Int. Edn Engl.* **37** 2202

[68] Kunieda H, Nakamura K and Evans D F 1991 *J. Am. Chem. Soc.* **113** 1051
[69] Kunieda H, Nakamura K, Infante M R and Solans C 1992 *Adv. Mater.* **4** 291
[70] Kunieda H, Nakamura K, Olsson U and Lindman B 1993 *J. Phys. Chem.* **97** 9525
[71] Mays H, Almgren M, Dedinaite A and Claesson P M 1999 *Langmuir* **15** 8072
[72] Schrage S, Sigel R and Schlaad H 2003 *Macromolecules* **36** 1417
[73] Diat O and Roux D 1993 *J. Physique* II **3** 9
[74] Diat O, Nallet F and Roux D 1993 *J. Physique* II **3** 1427
[75] Panizza P, Colin A, Coulon C and Roux D 1998 *Eur. Phys. J.* B **4** 65
[76] Montalvo G, Rodenas E and Valiente M 1998 *J. Colloid Interface Sci.* **202** 232
[77] Bergmeier M, Gradzielski M, Hoffmann H and Mortensen K 1999 *J. Phys. Chem.* B **103** 1605
[78] Bergenholtz J and Wagner N J 1996 *Langmuir* **12** 3122
[79] Hervé P, Roux D, Bellocq A M, Nallet F and Gulik-Krzywicki T 1993 *J. Physique* II **3** 1255
[80] van der Werff J C, de Kruif C G and Dhont J K G 1989 *Physica* A **160** 205
[81] van der Werff J C and de Kruif C G 1989 *J. Rheol.* **33** 421
[82] de Haas K H, Bloom C, van den Ende M H G, Duits B, Haveman B and Mellema J 1997 *Langmuir* **13** 6658
[83] Bergmeier M, Gradzielski M, Hoffmann H and Mortensen K 1998 *J. Phys. Chem.* B **102** 2837
[84] Bergenholtz J and Wagner N J 1996 *Langmuir* **12** 3122
[85] Escalante J I, Gradzielski M, Hoffmann H and Mortensen K 2000 *Langmuir* **16** 8653
[86] Bergenhausen J, Zipfel J, Diat O, Narayanan T and Richtering W 2000 *Phys. Chem. Chem. Phys.* **2** 2623
[87] Watanabe K, Nakama Y, Yanaki T and Hoffmann H 2001 *Langmuir* **17** 7219
[88] Mendes E, Narayanan J, Oda R, Kern F, Candau S J and Manohar C 1997 *J. Phys. Chem.* B **101** 2256
[89] Mendes E, Oda R, Manohar C and Narajanan J 1998 *J. Phys. Chem.* B **102** 338
[90] Richtering W 2001 *Curr. Opin. Colloid Interface Sci.* **6** 446
[91] Ninham B W, Evans D F and Wei G J 1983 *J. Phys. Chem.* **87** 5020
[92] Brady J E, Evans D F, Kachar B and Ninham B W 1984 *J. Am. Chem. Soc.* **106** 4279
[93] Talmon Y, Evans D F and Ninham B W 1983 *Science* **221** 1047
[94] Hoffmann H, Gräbner D, Hornfeck U and Platz G 1999 *J. Phys. Chem.* B **103** 611
[95] Gebicki J M and Hicks M 1973 *Nature* **243** 232
[96] Gebicki J M and Hicks M 1976 *Chem. Phys. Lipids* **16** 142
[97] Hargreaves J W and Deamer D W 1978 *Biochemistry* **17** 3759
[98] Watanabe K, Nakama Y, Yanaki T and Hoffmann H 2001 *Langmuir* **7219** 7224
[99] Kamenka N, Chorro M, Talmon Y and Zana R 1992 *Colloids Surf.* **67** 213
[100] Kaler E W, Murthy A K, Rodriguez B E and Zasadzinski J A N 1989 *Science* **245** 1371
[101] Kaler E W, Herrington K L, Murthy A K and Zasadzinski J A N 1992 *J. Phys. Chem.* **96** 6698
[102] Herrington K L, Kaler E W, Miller D D, Zasadzinski J A N and Chiruvolu S 1993 *J. Phys. Chem.* **97** 13792
[103] Yatcilla M T, Herrington K L, Brasher L L, Kaler E W, Chiruvolu S and Zasadzinski J A N 1996 *J. Phys. Chem.* **100** 5874
[104] Fukuda H, Kawata K and Okuda H 1990 *J. Am. Chem. Soc.* **112** 1635
[105] Ambühl M, Bangerter F, Luisi P L, Skrabal P and Watzke H J 1993 *Langmuir* **9** 36
[106] Kondo Y, Uchiyama H, Yoshino N, Nishiyama K and Abe M 1995 *Langmuir* **11** 2380
[107] Dubois M, Demé B, Gulik-Krzywicki T, Dedieu J C, Vautrin C, Désert S, Perez E and Zemb T 2001 *Nature* **411** 672
[108] Chen L, Xiao J X, Ruan K and Ma J 2002 *Langmuir* **18** 7250
[109] Kihara K, Tamori K, Esumi K and Meguro K 1993 *J. Japan. Oil Chem. Soc.* **42** 140
[110] Szönyi S and Watzke H J 1993 *Prog. Colloid Polym. Sci.* **93** 364
[111] Esumi K 1994 *Colloids Surf.* **84** 49
[112] Regev O and Khan A 1996 *J. Colloid Interface Sci.* **182** 95
[113] Kondo Y, Uchiyama H, Yoshino N, Nishiyama K and Abe M 1995 *Langmuir* **11** 2380
[114] Marques E F, Regev O, Khan A, da Graça Miguel M and Lindman B 1998 *J. Phys. Chem.* B **102** 6746
[115] Marques E F, Regev O, Khan A, da Graça Miguel M and Lindman B 1999 *J. Phys. Chem.* B **103** 8353
[116] Caria A and Khan A 1996 *Langmuir* **12** 6282
[117] Bhattacharya S and De S 1999 *Langmuir* **15** 3400
[118] Tondre C and Caillet C 2001 *Adv. Colloid Interface Sci.* **93** 115
[119] Watzke H J 1993 *Prog. Colloid Polym. Sci.* **93** 15
[120] Söderman O, Herrington K L, Kaler E W and Miller D D 1997 *Langmuir* **13** 5531
[121] Hentze H P, Raghavan S R, McKelvey C A and Kaler E W 2003 *Langmuir* **19** 1069
[122] Brasher L L, Herrington K L and Kaler E W 1995 *Langmuir* **11** 4267
[123] Mishra B K, Samant S D, Pradhan P, Mishra S B and Manohar C 1993 *Langmuir* **9** 894

[124] Hassan P A, Narayanan J, Menon S V G, Salkar R A, Samant S D and Manohar C 1996 *Colloids Surf.* A **117** 89
[125] Hassan P A, Valaulikar B S, Manohar C, Bourdieu L, Kern F and Candau S J 1996 *Langmuir* **12** 4350
[126] Lin Z, Chai J J, Scriven L E and Davis H T 1994 *J. Phys. Chem.* **98** 5984
[127] Buwalda R T, Stuart M C A and Engberts J B F N 2000 *Langmuir* **16** 6780
[128] Horbaschek K, Hoffmann H and Thunig C 1998 *J. Colloid Interface Sci.* **206** 439
[129] Narayanan J, Mendes E and Manohar C 2002 *Int. J. Mod. Phys.* **16** 375
[130] Regev O, Leaver M S, Zhou R and Puntambekar S 2001 *Langmuir* **17** 5141
[131] Jonströmer M and Strey R 1992 *J. Phys. Chem.* **96** 5993
[132] Olsson U, Nakamura K, Kunieda H and Strey R 1996 *Langmuir* **12** 3045
[133] Hofland H E J, Bouwstra J A, Gooris G S, Spies F, Talsma H and Junginger H E 1993 *J. Colloid Interface Sci.* **161** 366
[134] Montalvo G, Rodenas E and Valiente M 2000 *J. Colloid Interface Sci.* **227** 171
[135] Würtz J and Hoffmann H 1995 *J. Colloid Interface Sci.* **175** 304
[136] Auguste F, Douliez J P, Bellocq A M, Dufourc E J and Gulik-Krzywicki T 1997 *Langmuir* **13** 666
[137] Gomati R, Appell J, Bassereau P, Marignan J and Porte G 1987 *J. Phys. Chem.* **91** 6203
[138] Strey R, Schomäcker R, Roux D, Nallet F and Olsson U 1990 *J. Chem. Soc. Faraday Trans.* **86** 2253
[139] Jönsson B and Wennerström H 1987 *J. Phys. Chem.* **91** 338
[140] Munkert U, Hoffmann H, Thunig C, Meyer H W and Richter W 1992 *Langmuir* **8** 2629
[141] Thunig C, Platz G and Hoffmann H 1992 *Ber. Bunsenges. Phys. Chem.* **96** 667
[142] Radlinska E Z, Ninham B W, Dalbiez J P and Zemb Th 1990 *Colloids Surf.* **46** 213
[143] Schepers F J, Toet W K and Van de Pas J C 1993 *Langmuir* **9** 956
[144] Ristori S, Appell J and Porte G 1996 *Langmuir* **12** 686
[145] Okamura H, Imae T, Takagi K, Sawaki Y and Furusaka M 1996 *J. Colloid Interface Sci.* **180** 98
[146] Hoffmann H, Munkert U, Thunig C and Valiente M 1994 *J. Colloid Interface Sci.* **163** 217
[147] Wärnheim T, Bergenstahl B, Henriksson U, Malmvik A C and Nilsson P 1987 *J. Colloid Interface Sci.* **118** 233
[148] Regev O and Khan A 1994 *Prog. Colloid Polym. Sci.* **97** 298
Regev O, Kang C and Khan A 1994 *J. Phys. Chem.* **98** 6619
[149] Platz G, Thunig C, Pölike J, Kirchhoff W and Nickel D 1994 *Colloids Surf.* A **88** 113
[150] Joannic R and Auvray L 1997 *Phys. Rev. Lett.* **78** 3402
[151] Takeoka S, Mori K, Ohkawa H, Sou K and Tsuchida E 2000 *J. Am. Chem. Soc.* **122** 7927
[152] Lin Z, He M, Scriven L E, Davis H T and Snow S A 1993 *J. Phys. Chem.* **97** 3571
[153] Tedesco M M, Ghebremariam B, Sakai N and Matile S 1999 *Angew. Chem. Int. Edn* **38** 540
[154] Sidorov V, Douglas T, Dzekunov S M, Abdallah D, Ghebremariam B, Roepe P D and Matile S 1999 *Chem. Commun.* 1429
[155] Wang X F, Shen Y Z, Pan Y, Liang Y and Chu B 2000 *Langmuir* **16** 7538
[156] Bergmeier M, Gradzielski M, Thunig C and Hoffmann H 1988 *Nuovo Cimento* D **20** 2251
[157] Hoffmann H, Bergmeier M, Gradzielski M and Thunig C 1998 *Prog. Colloid Polym. Sci.* **109** 13
[158] Hao J, Hoffmann H and Horbaschek K 2000 *J. Phys. Chem.* B **104** 10144
[159] Hoffmann H, Horbaschek K and Hao J 2001 *Stud. Surf. Sci. Catal.* **132** 69
[160] Horbaschek K, Gradzielski M and Hoffmann H 2002 *Adsorption and Aggregation of Surfactants in Solution* ed K Mittal and D Shah (New York: Dekker)
[161] Laughlin R G 1997 *Colloids Surf.* A **128** 27
[162] Cantu L, Corti M, Musolino M and Salina P 1990 *Europhys. Lett.* **13** 561
[163] Cantu L, Corti M, Musolino M and Salina P 1991 *Prog. Colloid Polym Sci.* **84** 21
[164] Cantu L, Corti M, Del Favero E and Raudino A 1994 *J. Physique* II **4** 1585
[165] Gradzielski M, Hoffmann H, Horbaschek K and Witte F 2001 *Stud. Surf. Sci. Catal.* **132** 589
[166] Choucair A A, Kycia A H and Eisenberg A 2003 *Langmuir* **19** 1001
[167] Kawasaki H, Souda M, Tanaka S, Nemoto N, Karlsson G, Almgren M and Maeda H 2002 *J. Phys. Chem.* B **106** 1524
[168] Helfrich W 1986 *J. Physique* **47** 321
[169] Morse D C and Milner S T 1995 *Phys. Rev.* E **52** 5918
[170] Bergström M and Eriksson J C 1998 *Langmuir* **14** 288
[171] Safran S A, MacKintosh F C, Pincus P A and Andelman D A 1991 *Prog. Colloid Polym. Sci.* **84** 3
[172] Safran S A, Pincus P A, Andelman D and MacKintosh F C 1991 *Phys. Rev.* A **43** 1071
[173] Bergström M 1996 *Langmuir* **12** 2454
[174] Bergström M 2001 *J. Colloid Interface Sci.* **240** 294

[175] Yuet P K and Blankschtein D 1996 *Langmuir* **12** 3802
[176] Yuet P K and Blankschtein D 1996 *Langmuir* **12** 3819
[177] Jung H T, Coldren B, Zasadzinski J A, Iampietro D J and Kaler E W 2001 *Proc. Natl Acad. Sci. USA* **98** 1353
[178] Simons B D and Cates M E 1992 *J. Physique* II **2** 1439
[179] Boltenhagen P, Kleman M and Lavrentovich O D 1994 *J. Physique* II **4** 1439
[180] Fournier J B and Durand G 1994 *J. Physique* II **4** 975
[181] Chiruvolu S, Warriner H E, Naranjo E, Idziak S H J, Rädler J O, Plano R J, Zasadzinski J A and Safinya C R 1994 *Science* **266** 1222
[182] Fournier J B and Galatola P 1997 *Europhys. Lett.* **39** 225
[183] Oberdisse J, Couve C, Appell J, Berret J F, Ligoure C and Porte G 1996 *Langmuir* **12** 1212
[184] Oberdisse J, Regev O and Porte G 1998 *J. Phys. Chem.* B **102** 1102
[185] Oda R, Bourdieu L and Schmutz M 1997 *J. Phys. Chem.* B **101** 5913
[186] Ricoul F, Dubois M, Zemb T and Plusquellec D 1998 *Eur. Phys. J.* B **4** 333
[187] Bergström M and Pedersen J S 2000 *J. Phys. Chem.* B **104** 4155
[188] Beck R, Gradzielski M, Horbaschek K, Shah S S, Hoffmann H and Strunz P 2000 *J. Colloid Interface Sci.* **221** 200
[189] Oberdisse J and Porte G 1997 *Phys. Rev.* E **56** 1965
[190] Oberdisse J 1998 *Eur. Phys. J.* B **3** 463
[191] Cevc G and Marsh D 1987 *Phospholipid Bilayers* (New York: Wiley)
[192] Blandamer M J, Briggs B, Cullis P M, Last P, Engberts J B F N and Kacperska A 1999 *J. Therm. Anal. Calorim.* **55** 29
[193] Blandamer M J, Briggs B, Cullis P M, Irlam K D, Engberts J B F N and Streefland L 2000 *Thermochim. Acta* **364** 173
[194] Mason P C, Gaulin B D, Epand R M, Wignall G D and Lin J S 1999 *Phys. Rev.* E **59** 3361
[195] Vincent J M and Skoulios A 1966 *Acta Crystallogr.* **20** 441
[196] Garidel P, Richter W, Rapp G and Blume A 2001 *Phys. Chem. Chem. Phys.* **3** 1504
[197] Feitosa E, Barreleiro P C A and Olofsson G 2000 *Chem. Phys. Lipids* **105** 201
[198] Alder B J and Wainwright T E 1957 *J. Chem. Phys.* **27** 1208
[199] Hoffmann H and Ulbricht W 1996 *Curr. Opin. Colloid Interface Sci.* **1** 726
[200] Seddon K M, Hogan J L, Warrender N A and Pebay-Peyroula E 1990 *Prog. Colloid Polym. Sci.* **81** 189
[201] Bohlin L, Ljusberg-Wahren H and Miezis Y 1985 *J. Colloid Interface Sci.* **103** 294
[202] Gradzielski M, Hoffmann H, Panitz J C and Wokaun A 1995 *J. Colloid Interface Sci.* **169** 103
[203] Haering G and Luisi P L 1986 *J. Phys. Chem.* **90** 5892
[204] Quellet C and Eicke H F 1986 *Chimia* **40** 238
[205] Scartazzini R and Luisi P L 1988 *J. Phys. Chem.* **92** 829
[206] Atkinson P J, Robinson B H, Howe A M and Pitt A R 1995 *Colloids Surf.* A **94** 231
[207] Shchipunov Y A and Shumilina E V 1996 *Colloid J.* **58** 117
[208] Terech P, Furman I and Weiss R G 1995 *J. Phys. Chem.* **99** 9558
[209] Hoffmann H, Thunig C, Schmiedel P and Munkert U 1994 *Langmuir* **10** 3972
[210] Lekkerkerker H N W 1989 *Physica* A **159** 319
[211] Winterhalter M and Helfrich W 1992 *J. Phys. Chem.* **96** 327
[212] Hao J, Hoffmann H and Horbaschek K 2001 *Langmuir* **17** 4151
[213] Alfara M C, Guerrero A F and Munoz J 2000 *Langmuir* **16** 4711
[214] Bergmeier M, Hoffmann H, Witte F and Zourab S 1998 *J. Colloid Interface Sci.* **203** 1
[215] Flory P J 1950 *J. Chem. Phys.* **18** 108
[216] Hoffmann H 1994 *Ber. Bunsenges. Phys. Chem.* **98** 1433
[217] van der Linden E and Dröge J H M 1993 *Physica* A **193** 439
[218] Roux D and Safinya C R 1988 *J. Physique* **49** 307
[219] Dubois M, Zemb T, Belloni L, Delville A, Levitz P and Setton R 1992 *J. Chem. Phys.* **96** 2278
[220] Hufnagel A, Horbaschek K and Gradzielski M 2003 *J. Colloid Interface Sci.* submitted
[221] Fontell K, Mandell L and Ekwall P 1968 *Acta Chem. Scand.* **22** 3209
[222] Gradzielski M, Bergmeier M, Müller M and Hoffmann H 1997 *J. Phys. Chem.* **101** 1719
[223] Fontell K 1990 *Colloid Polym. Sci.* **268** 264
[224] Hoffmann H, Thunig C, Schmiedel P and Munkert U 1995 *Faraday Discuss.* **101** 319
[225] Gradzielski M, Müller M, Bergmeier M, Hoffmann H and Hoinkis E 1999 *J. Phys. Chem.* B **103** 1416
[226] Carnahan N F and Starling K E 1969 *J. Chem. Phys.* **51** 635
[227] Müller M 2000 *Dissertation* Universität Bayreuth
[228] Marques E F, Regev O, Khan A, da Graca Miguel M and Lindman B 1999 *Macromolecules* **32** 6626

[229] Kobayashi H, Amaike M, Jung J H, Friggeri A, Shinkai S and Reinhoudt D N 2001 *Chem. Commun.* 1038
[230] Chen L, Shen H and Eisenberg A 1999 *J. Phys. Chem.* B **103** 9488
[231] Lang J, Auborn J J and Eyring E M 1972 *J. Colloid Interface Sci.* **41** 484
[232] Edwards K, Gustafsson J, Almgren M and Karlsson G 1993 *J. Colloid Interface Sci.* **161** 299
[233] Silvander M, Karlsson G and Edwards K 1996 *J. Colloid Interface Sci.* **179** 104
[234] Xia Y, Goldmints I, Johnson P W, Hatton T A and Bose A 2002 *Langmuir* **18** 3822
[235] Shioi A and Hatton T A 2002 *Langmuir* **18** 7341
[236] Jung H T, Lee S Y, Kaler E W, Coldren B and Zasadzinski J A 2002 *Proc. Natl Acad. Sci. USA* **99** 15318
[237] Schurtenberger P, Mazer N and Känzig W 1985 *J. Phys. Chem.* **89** 1042
[238] Egelhaaf S U and Schurtenberger P 1994 *J. Phys. Chem.* **98** 8560
[239] Egelhaaf S U and Schurtenberger P 1997 *Physica* B **234–236** 276
[240] Egelhaaf S U, Olsson U and Schurtenberger P 2000 *Physica* B **276** 326
[241] Egelhaaf S U and Schurtenberger P 1999 *Phys. Rev. Lett.* **82** 2804
[242] Leng J, Egelhaaf S U and Cates M E 2002 *Europhys. Lett.* **59** 311
[243] Demé B, Dubois M, Gulik-Krzywicki T and Zemb T 2002 *Langmuir* **18** 997
[244] Lesieur P, Kiselev M A, Barsukov L I and Lombardo D 2000 *J. Appl. Crystallogr.* **33** 623
[245] Campbell S E, Zhang Z, Friberg S E and Patel R 1998 *Langmuir* **14** 590
[246] Farquhar K D, Misran M, Robinson B H, Steytler D C, Morini P, Garrett P R and Holzwarth J F 1996 *J. Phys.: Condens. Matter* **8** 9397
[247] Brinkmann U, Neumann E and Robinson B H 1998 *J. Chem. Soc. Faraday Trans.* **94** 1281
[248] Robinson B H, Bucak S and Fontana A 2000 *Langmuir* **16** 8231
[249] Bucak S, Robinson B H and Fontana A 2002 *Langmuir* **18** 8288
[250] O'Connor A J, Hatton T A and Bose A 1997 *Langmuir* **13** 6931
[251] Narayanan T, Diat O and Bösecke P 2001 *Nucl. Instrum. Methods Phys. Res.* A **467** 1005
[252] Zemb T and Charpin P 1985 *J. Physique* **46** 249
[253] Schmölzer S, Gräbner D, Gradzielski M and Narayanan T 2002 *Phys. Rev. Lett.* **88** 258301
[254] Aniansson E A G and Wall S N 1974 *J. Phys. Chem.* **78** 1024
[255] Aniansson E A G, Wall S N, Almgren M, Hoffmann H, Kielmann I, Ulbricht W, Zana R, Lang J and Tondre C 1976 *J. Phys. Chem.* **80** 905
[256] Gradzielski M, Grillo I and Narayanan T 2003 *Proc. Self-Assembly—the Future* at press
[257] http://www.ill.fr/yellowbook/D22/D22_info/D22_stopped_flow/html/D22_sf_title.html
[258] Gräbner D, Gradzielski M and Grillo I 2001 *ILL Annual Report* p 74
[259] Gradzielski M, Bergmeier M, Hoffmann H, Müller M and Grillo I 2000 *J. Phys. Chem.* B **104** 11594
[260] Brandl M, Drechsler M, Bachmann D and Bauer K H 1997 *Chem. Phys. Lipids* **87** 65
[261] Brandl M, Drechsler M, Bachmann D, Tardi C, Schmidtgen M and Bauer K H 1998 *Int. J. Pharm.* **170** 187